LICENCE TO McMASTER UNIVERSITY

This Thesis has been written
[Thesis, Project Report, etc.]

by John Stephen Ash for
[Full Name(s)]
Undergraduate course number 4K6 at McMaster University under the supervision/direction of Dr. D.M. Shaw.

In the interest of furthering teaching and research, I/we hereby grant to McMaster University:

1. The ownership of 3 copy(ies) of this work;
2. A non-exclusive licence to make copies of this work, (or any part thereof) the copyright of which is vested in me/us, for the full term of the copyright, or for so long as may be legally permitted. Such copies shall only be made in response to a written request from the Library or any University or similar institution.

I/we further acknowledge that this work (or a surrogate copy thereof) may be consulted without restriction by any interested person.

Denis Shaw
Signature of Witness,
Supervisor

J. Stephen Ash
Signature of Student

April 24, 1987
date

(This Licence to be bound with the work)

THE CONCENTRATION AND DISTRIBUTION OF BORON
IN THE KEWEENAWAN METABASALTS OF
MAMAINSE POINT, ONTARIO

THE CONCENTRATION AND DISTRIBUTION OF BORON IN THE KEWEENAWAN METABASALTS OF MAMAINSE POINT, ONTARIO

By

JOHN STEPHEN ASH

Submitted to the Department of Geology
in Partial Fulfilment of the Requirements
for the Degree
Bachelor of Science

April, 1987

BACHELOR OF SCIENCE (1987) (Geology)	McMASTER UNIVERSITY Hamilton, Ontario

TITLE: The concentration and distribution of boron in the Keweenawan metabasalts of Mamainse Point, Ontario

AUTHOR: John Stephen Ash

SUPERVISOR: Denis M. Shaw

NUMBER OF PAGES: i - xi; 1 - 93

ABSTRACT

Nine rock samples from the mafic volcanics of Mamainse Point, Ontario were analysed for boron using Prompt Gamma Neutron Activation Analysis (PGNAA) and Alpha-Track Imaging (ATI). The mean concentration of boron in these rocks was 7.85 ppm with a maximum concentration of 15.5 ppm and a minimum concentration of 4.21 ppm. The Mamainse Point samples are therefore enriched in boron relative to fresh basalts (∼ 2 ppm B) but depleted relative to basalts altered on the seafloor (30 - 60 ppm B). From ATI the boron was found to be most highly concentrated in iron oxides, chlorite, stilpnomelane and microscopic fractures throughout the rock. Plagioclase, clinopyroxene, quartz and calcite were all low in boron.

These results led to the conclusion that the Mamainse Point Formation is of continental rather than marine origin. The addition of boron to the rock has resulted from penecontemporaneous burial and hydrothermal metamorphism in the zeolite and subgreenschist facies through the interaction of boron-bearing hydrothermal fluids. The source of the boron is thought to be from the surrounding Precambrian terrain (Canadian Shield), the lower continental crust and magmatic fluids associated with volcanism.

ACKNOWLEDGEMENTS

I would like to thank Dr. D.M. Shaw without whom this project would not have been possible. I would also like to express my appreciation for valuable assistance and discussion from Dr. M.G. Truscott and T.A. Middleton. Many thanks are owed to L. Hillier for typing the manuscript, J. Whorwood for the photography and L. Zwicker for thin section preparation.

I would also like to thank M. Scruton for being a good friend these past years and the rest of the "Main Street Jammers" (close but no cigar!).

Finally, a salute to the class of '87 -- Here's to a banner year!

TABLE OF CONTENTS

Page

LIST OF TABLES

LIST OF FIGURES

LIST OF PLATES

CHAPTER 1

INTRODUCTION

1.1 SCOPE OF THE PROBLEM

The origin of the volcanic sequence which outcrops at Mamainse Point, Ontario has been questioned in recent years. The lavas are known to have erupted in Keweenawan time as a result of crustal rifting. Boron has recently been used as an environmental indicator and it seemed likely that its abundance in the Mamainse Point mafic volcanics might provide insight into the question of a marine or non-marine origin for these rocks. Boron analyses also appeared to provide useful informtion pertaining to the alteration history of the lava sequence.

1.2 PREVIOUS WORK

The Mamainse Point Formation has been of interest to geologists and prospectors for over a century due to its native copper and silver deposits. Intense mining of this area began in 1965 but the economic mineral wealth has now diminished and mining activity has ceased.

The preliminary mapping of Mamainse Point and adjacent localities was carried out by Sir William Logan in 1863 for the newly established Geological Survey of Canada. More recent mapping was performed by P.E. Giblin in 1963. Detailed studies of stratigraphy, petrography and chemistry were carried out by R.N. Anells in 1973.

Other important works that were utilized in this project are geochemical studies of the Mamainse Point Formation by N.W.D. Massey in 1980, geophysics of the Keweenawan rift system by H.C. Halls in 1978, a review of Kewweenawan volcanism in the Lake Superior region by J.C. Green in 1977, and a discussion on boron geochemistry and distribution in the oceanic lithosphere by M. Bergeron in 1985.

This body of literature supplies the necessary background to complement the present study.

CHAPTER 2

THE GEOLOGY OF THE MAMAINSE POINT AREA

2.1 INTRODUCTION

The overall structure of the Keweenawan rocks of the Lake Superior region consists of a large arcuate geosyncline 2000 km long by 60 km wide. The axis of the belt trends through Lake Superior from the southwest corner to the southeast. Several reverse faults occur which modify this structure (Green, 1982). A geological map of the area is presented in Figure 2.1 (after Halls, 1978).

Traditionally thought to have accumulated in the elongate Lake Superior syncline, several recent studies have proclaimed that these rocks are a product of crustal rifting (King and Zietz, 1970). Sialic crustal rocks have been replaced by denser material with seismic velocities of 6.5-6.9 km/sec. Evidence for the rifting hypothesis has been presented by Halls (1978):

(a) The Keweenawan rift has similar dimensions to the East African rift and the Red Sea,

(b) flood basalts fed by the fissure system have a

Figure 2.1 Geological Map of the Central North American Rift System, with Paleozoic and surficial cover removed (after Halls, 1978).

<u>Legend</u>

1. Geological Contact
2. Structural Form Lines
3. Synclinal axis
4. Fault
5. Boundary of Keweenawan volcanics
6. Northern Limit of Paleozoic cover
7. Boreholes which penetrate
    a) Keweenawan mafic igneous rocks
    b) Keweenawan red clastics and underlying mafics
    c) red clastics only
    d) red clastics and underlying pre-Keweenawan basement
    e) basement only
8. Grenville front
9. Keweenawan diabase dyke swarm
10. Keweenawan volcanics and extrusives (I) within the rift zone
11. Keweenawan red clastics

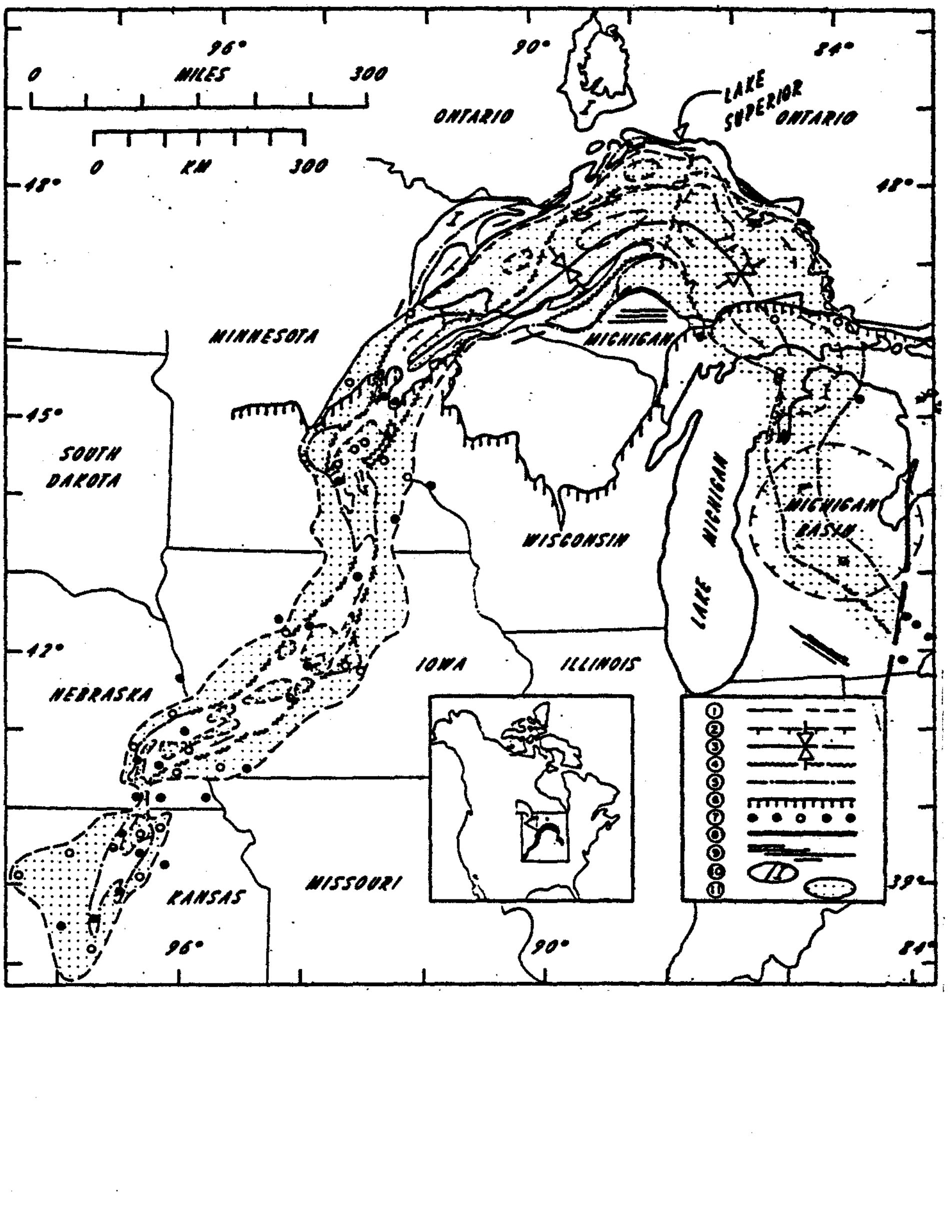
96°
0
MILES
300
90°
84°
ONTARIO
LAKE SUPERIOR
ONTARIO
0
KM
300
48°
48°
MINNESOTA
MICHIGAN
45°
SOUTH DAKOTA
WISCONSIN
LAKE MICHIGAN
MICHIGAN BASIN
42°
IOWA
ILLINOIS
NEBRASKA
KANSAS
MISSOURI
39°
96°
90°
84°
①
②
③
④
⑤
⑥
⑦
⑧
⑨
⑩
⑪

trend which is parallel to the axis of the belt,

(c) granitic crust is absent beneath the central part of the belt with the crust beneath Lake Superior and the Mid-Continental Geophysical Anomaly being mafic in composition, and,

(d) the Keweenawan belt has been widened due to crustal spreading from an axial zone of dyke injection.

The Keweenawan rift complies to the definition proposed by Burke (1978): "an elongate depression overlying places where the entire thickness of the lithosphere has been ruptured in extension". The cause for rifting is still in a state of flux but several hypotheses have been proposed. These are:

(a) Plume generated rifting (Burke and Dewey, 1973),

(b) Opening of the Grenvillian Proto-Atlantic Ocean (Burke and Dewey, 1973),

(c) Rifting due to Grenville shearing (McWilliams and Dunlop, 1978),

(d) Rifting related to the Grenville collision event (Sawkins, 1976).

Green (1977, 1982) has summarized the history and nature of the volcanism of the Keweenawan plateau and Lake Superior district. In Keweenawan time, the region now occupied by Lake Superior was a broad, barren volcanic plateau. The volcanism was primarily fissure-type with isolated shields enveloped by basaltic flows. Dyke swarms representing the feeder conduits of the system, cut through older rocks beyond the present extent of the lavas and also parts of the lower portions of many of the lava accumulations. There is no evidence that a valley existed in the region when the volcanism began and apparently the lavas outpoured onto a relatively flat surface. The basal flows either overlie eroded bedrock, as at Mamainse Point, or were deposited in a shallow water environment that had low relief and deposited quartz-arenite, as at the southern flank of Wisconsin and Michigan.

Volcanism occurred in a series of overlapping lava plateaus (Table 2.1) on the order of 250 x 130 km in extent (Green, 1982). Approximately 400,000 km of volcanic material were ejected in the Lake Superior region, and therefore crustal subsidence would have to play a vital role to accommodate this volume (Halls, 1978). Green (1982) confirms that within each plateau accumulation, gentle subsidence took place during and/or after eruption. Due to the fact that little or no erosion took place, a continuous record of volcanic activity has been preserved.

Therefore, the development of the Lake Superior basin began with local subsidence occurring within active volcanic areas (Green, 1982). The basin continued to form

Table 2.1 Keweenawan Lava Plateaus of the Lake Superior region. Magnetic polarities and individual thicknesses of the units comprising each plateau have been indicated (after Massey, 1980)

STAGE	LAVA PLATEAU	THICKNESS (km)	MAGNETIC POLARITY
4	Keweenaw Point - Isle Royale	2.5 - 5.2	normal
	Keweenaw Point	2.4 - 5.2	
	Isle Royale	3.1	
3	North Shore	3.7 - 7.1	normal
	Mamainse - Michipicoten	4.1 - 5.1	normal
	Maimainse Point	2.6	
	Michipicoten Island	2.5	
	Osler	0.1+	normal
2	Mamainse Point - Alona Bay	2.5	reversed
	Osler	2.75	reversed
	Ironwood - Grand Portage - Nopeming	3.0 - 6.3	reversed
	Powdermill Group	2.4 - 5.1	
	Grand Portage - Hovland	2.7 - 3.0	
	Ely's Peak	0.4	
1	Siemens Creek	0.12	normal

as a result of loading and isostatic adjustment throughout the remainder of Proterozoic time.

The Keweenawan sequence at Mamainse Point, Ontario lies at the eastern end of Lake Superior and rests unconformably on Archean granitic rocks, metasediments and metavolcanics of the Superior province which has an age greater than 2.5 billion years (Annells, 1973). A geological map of Mamainse Point Formation is presented in Figure 2.2. The sequence is dominated by the Mamainse Point Formation which consists of mafic flows, felsic intrusions and interlayered clastic sediments (Massey, 1980). The flows are predominantly basalts of tholeiitic composition (Fig. 2.3). No intermediate rocks have been observed. The basalts strike north to northwest and dip westerly towards Lake Superior at 15-45°.

The Mamainse Point and Alona Bay flows are overlain to the north by conglomerate, arkosic sandstones and shales of upper Keweenawan age (Annells, 1973). The sandstones of the Jacobsville group are in fault contact with the Mamainse Point Formation to the south (Massey, 1980).

The rocks from Mamainse Point have been dated by K/Ar, Rb/Sr and paleomagnetic studies and have an age of 1.0 to 1.2 billion years.

Figure 2.2 Geological Map of the Mamainse Point area (after Giblin, 1969).

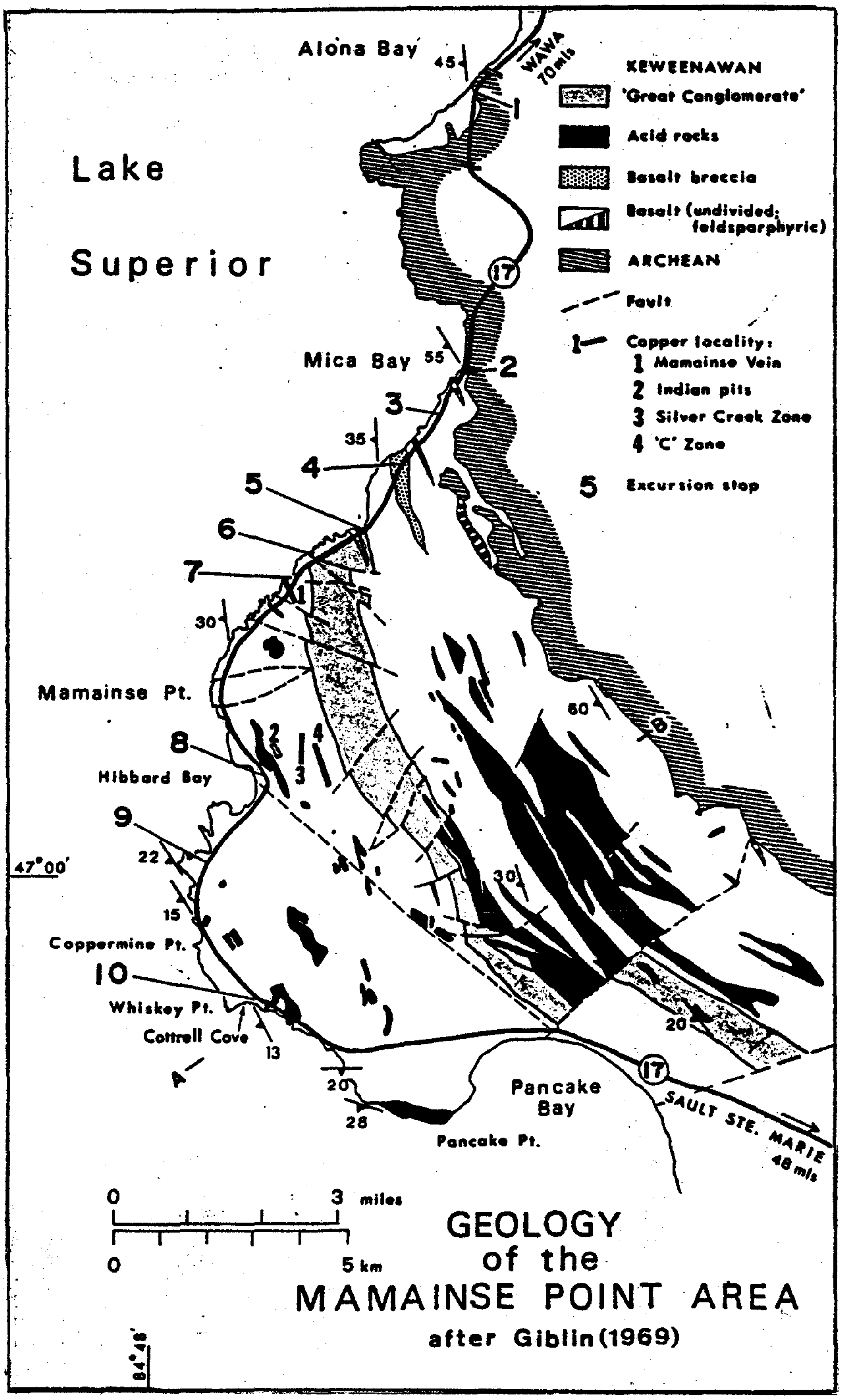

GEOLOGY of the MAMAINSE POINT AREA after Giblin (1969)

Figure 2.3 AFM plot of the Mamainse Point Keweenawan volcanic rocks. Symbols on the diagram define provenance of the data points including Mamainse Point lava series, Alona Bay flows and dykes. (Tholeiitic-calc-alkaline boundary after Irvine and Baragar, 1971; analyses by Massey, 1980.)

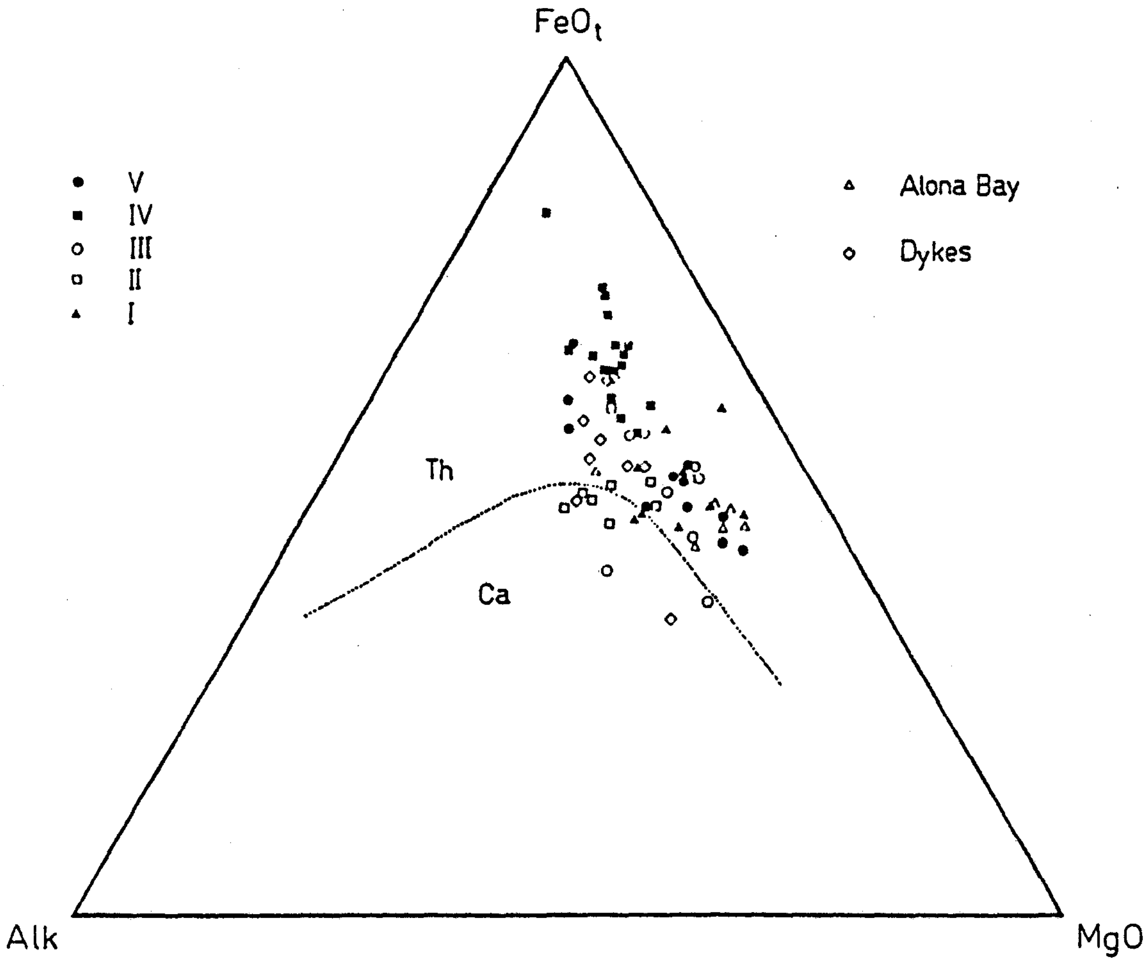
FeO$_t$
Alk
MgO
● V
■ IV
○ III
□ II
▲ I
△ Alona Bay
◇ Dykes
Th
Ca

2.2 FIELD CHARACTERISTICS OF THE MAMAINSE POINT FORMATION

2.2.1 Introduction

The Mamainse Point Formation is similar to basalt provinces elsewhere in space and time (Annells, 1973). The lavas are chemically bimodal and consist of basaltic and rhyolitic types. They have been extruded onto a surface which was susceptible to intermittent subsidence and flooding as evidenced by the presence of intercalated sedimentary horizons (Annells, 1973). The red colour of the horizons indicate an arid paleoclimate (Schwarzbach, 1963).

The basal parts of some of the flows are brecciated into vessicular fragments and are often mixed with silty material where the flows rest on conglomerate horizons (Annells, 1973). This feature is produced by rapid, explosive volatilization of small pools of water lying on the conglomerate when it was crossed by the advancing flow. The contact of the basal Mamainse Point flows with the underlying Archean rocks shows poor exposure, but when it can be observed it is undulating.

The Mamainse Point type section lies between Mica Bay and Pancake Bay as defined by Annells (1973). It represents the lowest part of the Keweenawan volcanic pile with the base outcropping at Alona Bay. The total thickness of the formation, including the member on Michipicoten

Island, is approximately 6,800 m (Annells, 1973). However, in the area of study, the thickest succession is 5,988 m but this thickness may be complicated by faulting and dialation of the basaltic pile by felsic intrusions (Massey, 1980).

Annells (1973) made a crude stratigraphic subdivision of the sequence into two divisions separated by the Great Conglomerate.

2.2.2 Mafic Volcanics

70% of the Mamainse Point Formation consists of basaltic flows (Fig. 2.4). Over 300 individual flows have been counted and these have variable thickness ranging between 1.5 and 9.0 m on average but rarely obtaining a thickness of 30 m (Massey, 1980).

The thicker flows have thin flow units (approx. 15 cm) representing pulses of one eruption (Nicholls, 1936 in Massey, 1980). These thin flows have lower zones bearing vesicles and upper ropey pahoehoe surfaces.

The basaltic flows had quite a low viscosity as evidenced by well preserved wrinkled and ropey pahoehoe surfaces (Annells, 1973). Some flows however show scoriaceous tops with an infilling of red-brown dust. All flows show development of amygdaloidal tops which are often oxidized. Vesicles are generally rounded and up to 2.5 cm in diameter. They may be slightly flattened in the upper

Figure 2.4 Stratigraphy of the Mamainse Point area
(after Smith, 1974 in Massey, 1980).

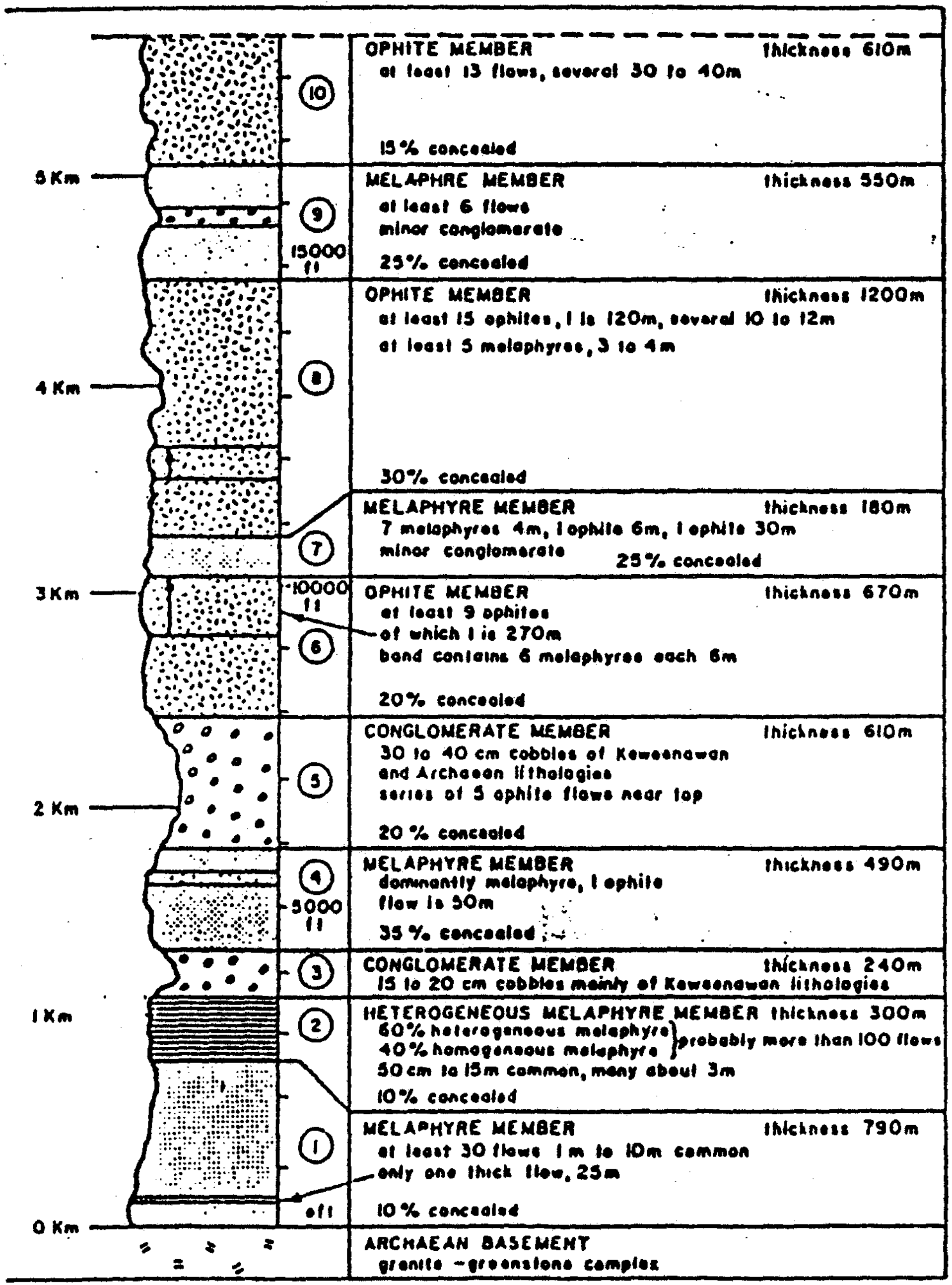

OPHITE MEMBER thickness 610m
at least 13 flows, several 30 to 40m
15% concealed

MELAPHRE MEMBER thickness 550m
at least 6 flows
minor conglomerate
25% concealed

OPHITE MEMBER thickness 1200m
at least 15 ophites, 1 is 120m, several 10 to 12m
at least 5 melaphyres, 3 to 4m
30% concealed

MELAPHYRE MEMBER thickness 180m
7 melaphyres 4m, 1 ophite 6m, 1 ophite 30m
minor conglomerate 25% concealed

OPHITE MEMBER thickness 670m
at least 9 ophites
of which 1 is 270m
band contains 6 melaphyres each 6m
20% concealed

CONGLOMERATE MEMBER thickness 610m
30 to 40 cm cobbles of Keweenawan
and Archaean lithologies
series of 5 ophite flows near top
20 % concealed

MELAPHYRE MEMBER thickness 490m
dominantly melaphyre, 1 ophite
flow is 50m
35 % concealed

CONGLOMERATE MEMBER thickness 240m
15 to 20 cm cobbles mainly of Keweenawan lithologies

HETEROGENEOUS MELAPHYRE MEMBER thickness 300m
60% heterogeneous melaphyre
40% homogeneous melaphyre } probably more than 100 flows
50 cm to 15m common, many about 3m
10% concealed

MELAPHYRE MEMBER thickness 790m
at least 30 flows 1m to 10m common
only one thick flow, 25m
10 % concealed

ARCHAEAN BASEMENT
granite – greenstone complex

part of the flow or take on an irregular appearance in the central part (Massey, 1980).

Basal pipe vesicles are common in many flows and may be inclined in the direction of flow movement. The vesicles are all filled with chlorite, calcite, quartz and other secondary minerals.

Two main textural rock types occur in the Mamainse Point mafic flows. These are Ophites and Melaphyres.

The ophites have a mottled appearance (Annells, 1973) due to large, spheroidal augite grains poikilitically enclosing plagioclase laths (Massey, 1980). The mottles are 5 mm to 2 mm across. The ophites range from dark grey to red in colour and show either spheroidal or crumbly weathering (Massey, 1980). They comprise 81% of the Mamainse Point flows and 89% of the Alona Bay flows.

The melaphyres are very fine-grained and many minerals are undiscernable to the naked eye. They may show some interstitial mesostatic glassy material. These flows are generally fractured and splintery in appearance and weather to angular blocks (Massey, 1980). The melaphyres comprise 19% and 11% of the Mamainse Point and Alona Bay flows, respectively.

A less common mineralogy in the mafic flows is diabasic, where augite and plagioclase grains 2 to 4 mm in size form an intergranular or gabbroic texture (Annells, 1973; Massey, 1980).

The Daisy Stone flow is the most distinctive lithology of the formation (see Plate 3). It occurs 195 m above the base of the section (Annells, 1973) and consists of radiating clusters of plagioclase with interstitial augite in a fine-grained matrix. This is called glomerophitic texture. Similar flows occur at Cape Gargantua (64 km north of Mica Bay) and in Michigan. Both flows are associated with a group of tholeiitic flows rich in phenocrystal olivine pseudomorphs comprising 35% (by volume) of some of the Mica Bay flows (Annells, 1971). Both flows represent the simultaneous eruption of the same mafic magma supply over a very large area.

Mafic dykes are rare in the Mamainse Point and Alona Bay sections (Massey, 1980). They are usually grey, medium-grained, diabasic rocks. The dykes are usually about 1 m wide and show chilled margins, perpendicular, prismatic jointing and occasional small vesicles (Massey, 1980). They usually cut across the flows at a steep angle (Massey, 1980). The scarcity of the dykes reflects the position of the Mamainse Point Formation relative to the rift; it overlaps onto the sialic basement being close to the edge of the rift. Ropey tops and pipe vesicles indicate that most of the flows had sources further southwest in more axial regions of the rift beneath the present position of Lake

Superior (Massey, 1980). Mafic dykes also cut across Archean rocks; however, these are different from the dykes which cut through the Mamainse Point Formation (Massey, 1980).

2.2.3 Felsic Volcanics

Three main types of acidic rocks occur in the Mamainse Point Formation. These are quartz porphyries, felsites and flow banded rhyolite. The thickest bodies are stratiform and occur in the central parts of the area near Pancake Point (Massey, 1980).

The acid rocks are too sialic in nature to represent straightforward differentiates of a basaltic magma (Annells, 1973). They are similar in composition to the quartz-latite range of the Minnesota North Shore Group (Green, 1971) and are fine-grained with "tough, compact, flinty or rough, granular texture" (Annells, 1973). Many of the small bodies show well developed flow lamination at their margins resulting in platy fracture (Annells, 1973).

The quartz-porphyries commonly occur as small plugs which are densely populated with quartz phenocrysts and altered, euhedral feldspar. Some opaque phenocrysts also occur in these rocks.

Annells (1973) pointed out that many of the rhyolitic sequences were injected before complete consolidation of the basic lining of the fissure. This would imply immiscibility between these two phases.

2.2.4 Intercalated Sediments

Coarse sandstones and conglomerates are quite abundant in the Mamainse Point Formation comprising about 15% of the section. They are rare in the Alona Bay flows. Massive, polymictic conglomerates can form horizons over 30 m thick with the Great Conglomerate reaching a thickness of 540 m. No conglomerate is present in the Alona Bay Formation (Annells, 1973).

The conglomerates contain clasts of greenstone, granite and gneiss which have been derived from the Archean highlands bordering the Keweenawan trough. The clasts are well rounded and may be 1.2 m in diameter. Clasts of Keweenawan basalt and rhyolite may also be found in the conglomerates. This led Annells (1973) to interpret them as "fanglomerates" (alluvial fans) which were deposited by short-lived streams flowing towards the centre of the basin. The conglomerates also have a red-brown, sand- to silt-size matrix which is sometimes concentrated into thin, well-stratified layers (Annells, 1973). These often show cross-bedding indicative of the "temporary development of a deltaic depositional environment" (Annells, 1973).

Paleocurrent studies by Merk and Jirsa (1982) indicate that the source area for the sediments was to the east of the present Keweenawan exposures. The composition, immaturity and coarseness of the interflow sediments indicate that the source was nearby and tectonically active throughout mid-Keweenawan time. Sedimentary structures such as cross-bedding, flute casts and grooves reflect basinward deposition patterns and that distribution of the sediments was controlled by the subsidence of the Lake Superior basin (Jirsa, 1978).

2.2.5 Metamorphism

The Mamainse Point and Alona Bay sequences have suffered low-grade hydrothermal and burial metamorphism (Jolly and Smith, 1972) which has affected the primary mineralogy leading to the formation of secondary minerals in vesicles and along fractures. Olivine was the first mineral to be affected an it has been pseudomorphed by saponite and hematite (Annells, 1973) and iddingsite. No fresh olivine remains in the Mamainse Point or Alona Bay flows.

Plagioclase laths may show saussuritization patches of albite and epidote.

Pyroxene may be altered to clinoamphibole and greenish chloritic material and Ca-poor pyroxene may show alteration to carbonate (Annells, 1973).

The opaques are mostly altered to hematite but Ti-rich oxides also exist.

Stilpnomelane occurs at all levels throughout the volcanic pile.

Chlorite occurs in vesicles which are lined with chalcedony. The vesicles may also contain prehnite, calcite and some quartz.

Epidote is generally restricted to the lower part of the sequence.

Pumpellyite was observed in thin section as an alteration product of plagioclase.

Native copper, introduced into hydrated rocks (Jolly, 1974) is reported to occur where pumpellyite, prehnite, laumontite and chlorite are the principal hydrous secondary phases. It occurs in the upper sections of the volcanic pile associated with epidote gangue (Massey, 1980).

Metamorphism of the Mamainse Point-Alona Bay flows has occurred in the zeolite to sub-greenschist facies regime. Metamorphic effects are most noticeable in flow tops and bottoms and along joint plane surfaces suggesting control by fluid pathways (Massey, 1980).

2.2.6 Geophysical Studies

Seismic and gravity studies show that the crust beneath the Keweenawan rift is unusually thick and dense. Beneath Lake Superior it may reach 45-50 km (Halls, 1978).

The observed seismic velocities of 6.5 to 6.9 km/sec are consistent with the lithology of the exposed metavolcanic sequences which outcrop around Lake Superior.

At least two paleomagnetic reversals have been recorded in these Keweenawan rock sequences (Books, 1972 in Davidson, 1982). Only at Mamainse Point does the reversal occur within a sequence of lavas (Massey, 1980). This feature is shown in Figure 2.5. Faulting may however complicate the situation. Paleomagnetic polarization sequences have considerable use for interregional correlation of rock units around the Lake Superior region and may even be recognizable on a worldwide scale making them valuable in long-distance correlation (Morey and Green, 1982).

The Keweenawan rift extends from the top of Lake Superior southwesterly towards Wisconsin and southeasterly from the top of Lake Superior to Michigan in two "arms". These form the U-shaped pattern of the "Logan's Loop". The northeast or northwest trends of faults in the Keweenawan rift may suggest that the shape of the rift is controlled by a pre-existing weakness (Halls, 1978). Thought to represent a triple junction feature, the failed arm of the Keweenawan rift is represented by the Kapuskasing fault zone which runs for more than 300 km in a southwest direction from Hudson Bay to the east shore of Lake Superior (Bennett, 1967). This

Figure 2.5 Stratigraphic correlation diagram for Keweenawan volcanic rocks and associated sediments of the Lake Superior area (after Green, 1977).

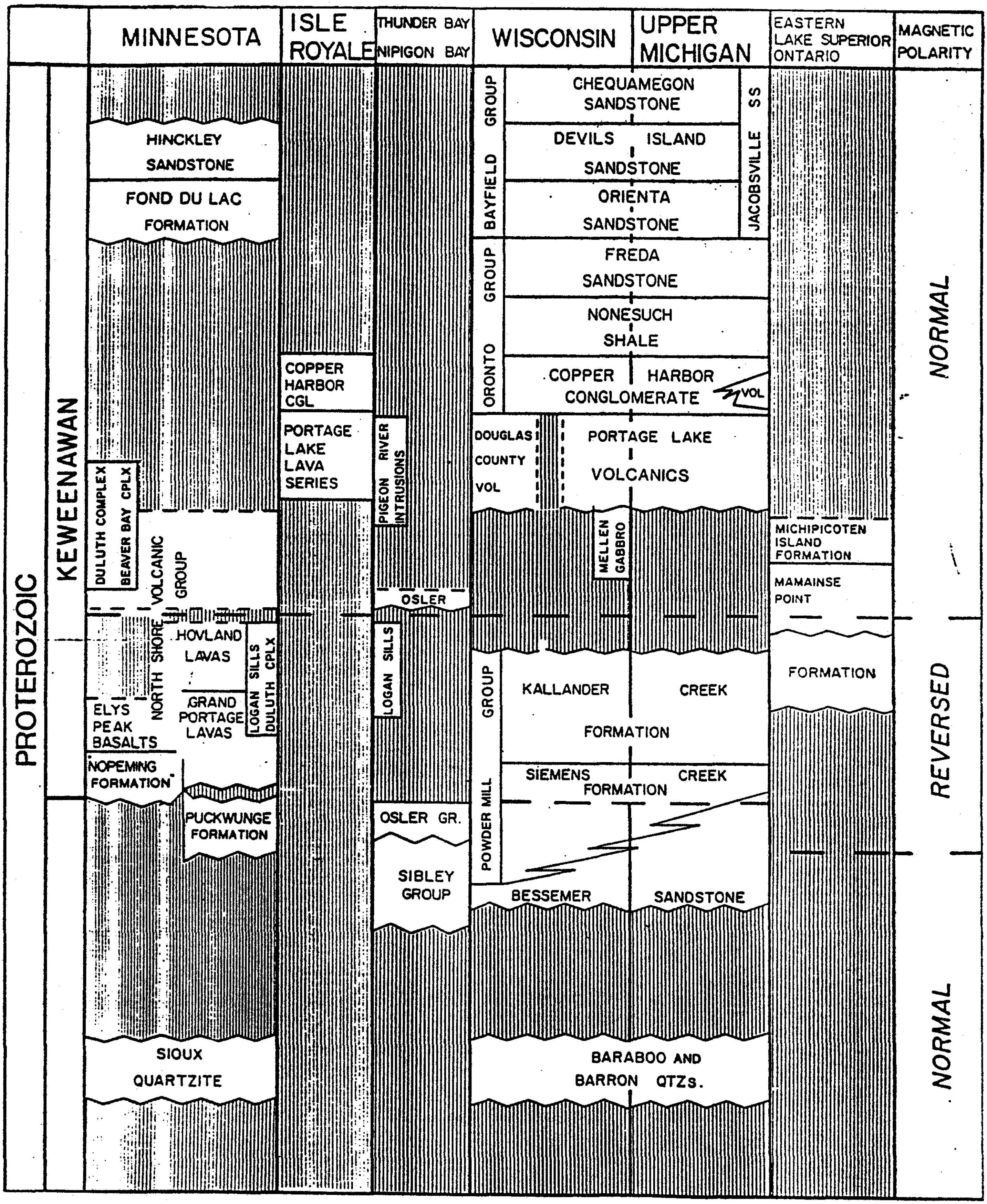
MINNESOTA
ISLE ROYALE
THUNDER BAY NIPIGON BAY
WISCONSIN
UPPER MICHIGAN
EASTERN LAKE SUPERIOR ONTARIO
MAGNETIC POLARITY
PROTEROZOIC
KEWEENAWAN
HINCKLEY SANDSTONE
FOND DU LAC FORMATION
DULUTH COMPLEX
BEAVER BAY CPLX
NORTH SHORE VOLCANIC GROUP
HOVLAND LAVAS
GRAND PORTAGE LAVAS
LOGAN SILLS
DULUTH CPLX
ELYS PEAK BASALTS
NOPEMING FORMATION
PUCKWUNGE FORMATION
SIOUX QUARTZITE
COPPER HARBOR CGL
PORTAGE LAKE LAVA SERIES
PIGEON RIVER INTRUSIONS
OSLER
LOGAN SILLS
OSLER GR.
SIBLEY GROUP
BAYFIELD GROUP
CHEQUAMEGON SANDSTONE
DEVILS ISLAND SANDSTONE
ORIENTA SANDSTONE
JACOBSVILLE SS
ORONTO GROUP
FREDA SANDSTONE
NONESUCH SHALE
COPPER HARBOR CONGLOMERATE
VOL
DOUGLAS COUNTY VOL
PORTAGE LAKE VOLCANICS
MELLEN GABBRO
POWDER MILL GROUP
KALLANDER CREEK FORMATION
SIEMENS CREEK FORMATION
BESSEMER SANDSTONE
BARABOO AND BARRON QTZS.
MICHIPICOTEN ISLAND FORMATION
MAMAINSE POINT FORMATION
NORMAL
REVERSED
NORMAL

hypothesis is however questionable because the fault is poorly developed at the southern end. An alternative for the failed arm of the triple junction is along a north-northwest line through Lake Nipigon (Halls, 1978). Here, considerable amounts of mafic magma were produced during the onset of Keweenawan volcanic activity. Within the rift a number of basins are arranged en echelon and each basin has developed its own stratigraphy independently of other basins (Halls, 1978; Massey, 1980). This led to a three-fold division of the Keweenawan Supergroup consisting of a Lower Sedimentary unit, a Middle Volcanic unit and an Upper Sedimentary unit.

2.3 SAMPLE SELECTION

N.W.D. Massey (1980) has made a detailed geochemical study of the Mamainse Point metabasites. His rock samples have been utilized in this project.

Al, Σ Fe, Mg, Ti, P, Y, Zr, Nb, Ni, Cr, Co, REEs, Th, Ta, Hf and U are apparently immobile or only moderately affected by alteration (Massey, 1980). Using the stratigraphic variation of these elements it is possible to divide the Mamainse Point Formation into five series. It was decided, due to time alottment, that only one metabasalt from each series and one each from the Alona Bay and Daisy

Stone flows could be studied in this experiment. (Two samples were actually taken from Series V for interest's sake, making a total of 9 samples to be studied.)

Petrographical analysis was used to determine the best samples for the project. The "best samples" were chosen on the basis of overall texture. Texture is especially important for the qualitative analysis (alpha-track imaging) because if the rock is too fine-grained observational difficulties are encountered. Therefore, the experiment will be slightly biased toward more coarsely grained samples.

The rock sample identification is shown in Table 2.2.

Table 2.2 Identification of the 9 samples which will be studied in this project (after Massey, 1980)

SAMPLE	UNIT FROM WHICH THE SAMPLE WAS DERIVED	STRATIGRAPHIC HEIGHT OF THE UNIT ABOVE BASE (m)
R95	Dyke	4333
R92	Series 5	3090 - 4367
R93	Series 5	3090 - 4367
R78	Series 4	2225 - 3227
R63	Series 3	1485 - 1733
R28	Series 2	400 - 1250
R18	Daisy Stone Flow	120 - 145
R19	Series 1	0 - 500
R105	Alona Bay Flow	*

Note: *indicates that the exact stratigraphic relationship of the Alona Bay Flow to the Mamainse Point Flows is unknown.

CHAPTER 3

ANALYTICAL METHODS AND RESULTS

3.1 PGNAA

3.1.1 Introduction

Prompt Gamma Neutron Activation Analysis (PGNAA) can be used to determine the concentration of certain elements in a powdered or crushed sample. Gamma-rays emitted from a sample can be detected and analysed using this method. PGNAA depends on the measurement of one or more products during a reaction. For example, one can write:

$$X(n,b)Y.$$

This means that nuclide X reacts with a neutron to form nuclide Y with the emission of b, where b = alpha-particles, beta-particles or gamma-rays.

This reaction will only proceed in principle if Y is radioactive (Peisach, 1981a, pg. 93). Only rarely does the stability of Y affect the analysis.

In the real sense, the reaction above produces the nuclide Y in an excited state. It is the subsequent decay of Y which emits the gamma-ray we can measure in PGNAA. The gamma-ray produced by the radioactive decay of each element is like a personal signature and may be used to qualitatively identify and quantitatively measure the presence of the element in the sample of interest.

PGNAA has many advantages over other analytical methods. It is fast, efficient and relatively simple and allows "on-the-spot" analysis. No rapid transfer equipment is necessary. PGNAA is a method of particular interest to this project because of the high capture cross-section of boron (752 barns) for thermal neutrons. Therefore, a crushed sample of approximately 2 grams can be analysed for boron with a good degree of precision and accuracy in as little as 10^3 - 10^4 seconds.

Upon thermal neutron bombardment, the reaction

$$^{10}B(n,\alpha)^{7}Li^{*}$$

occurs. $^{7}Li^{*}$ rapidly decays to ^{7}Li with the emission of a gamma-ray. Another way of stating the reaction is

$$^{10}B + n \longrightarrow {}^{7}Li + {}^{4}He + \gamma.$$

The emitted gamma-ray has an energy of 478 keV. The gamma-rays are usually detected with a Ge(Li) detector specially manufactured to be free of ^{10}B components. It is possible that the Al used in the manufacture of the detector is contaminated with boron; however, the effect is trivial in this project (Higgins et al., 1984). The detector is connected to a multi-channel analyser and display screen on which the gamma-spectrum of the sample may be imaged and analysed.

In this project it has been assumed that samples containing natural boron have constant $^{10}B/^{11}B$ and therefore the amount of ^{10}B in the samples reflects the proportional amount of natural boron in these rocks.

3.1.2 Sample Preparation

The samples had been previously crushed and powdered by Massey (1980) so that they were ready for sample preparation. The powdered samples were loaded into 7 cm by 1 cm tubular teflon capsules such that the powder depth within the capsule was approximately 3 cm. This depth ensures that the maximum amount of sample material is exposed to the neutron beam. The mass of the powder was weighed accurately but was about 2 grams on average. After loading, the teflon capsules were plugged with polyethylene disks.

3.1.3 PGNAA - The McMaster Facility

The neutron source for this experiment was the 2 MW pool-type nuclear reactor on the campus of McMaster University. It has a full neutron flux of 10^{13} ncm^{-2} s^{-1}. the neutrons are extracted from the source by way of a 15 cm diameter beam port which views the core of the reactor directly. However, the neutron beam must be filtered to remove the fast neutrons and gamma-rays which could seriously damage the detector and augment the gamma-ray background in the spectrum. Only thermal neutrons are required for the experiment. For this purpose, a combination of 60 cm of cylindrical silicon crystals (12 cm in diameter) are used (Higgins et al., 1984). The beam is initially collimated by lead and heavy concrete annuli and finally shaped by a rotatable shutter of polyethylene and lead. A tunnel of $^{6}LiCO_3$/wax connects the shutter to the beam stop (Fig. 3.1). After filtering and collimation the thermal neutron flux is 6 x 10^7 to 10^8 ncm^{-2} s^{-1} and the beam is rectangular in shape (2.5 cm by 5 cm).

The gamma-rays are detected using a Ge(Li) detector (APTEC) manufactured to be free of boron components. The detector is shielded from neutrons by a $^{6}LiCO_3$/wax cap which is 1 cm thick, a boraflex (borated rubber) sheet and 5-10 cm of a wax + concrete housing to optimize operation safety. This aparatus is shown in Figure 3.2.

3.1.4 Calibration

Calibration of the analytical system was achieved through the use of two materials of known boron concentration:

Figure 3.1 Cross-section of the beam port at the McMaster University Reactor (after Higgins *et al.*, 1984).

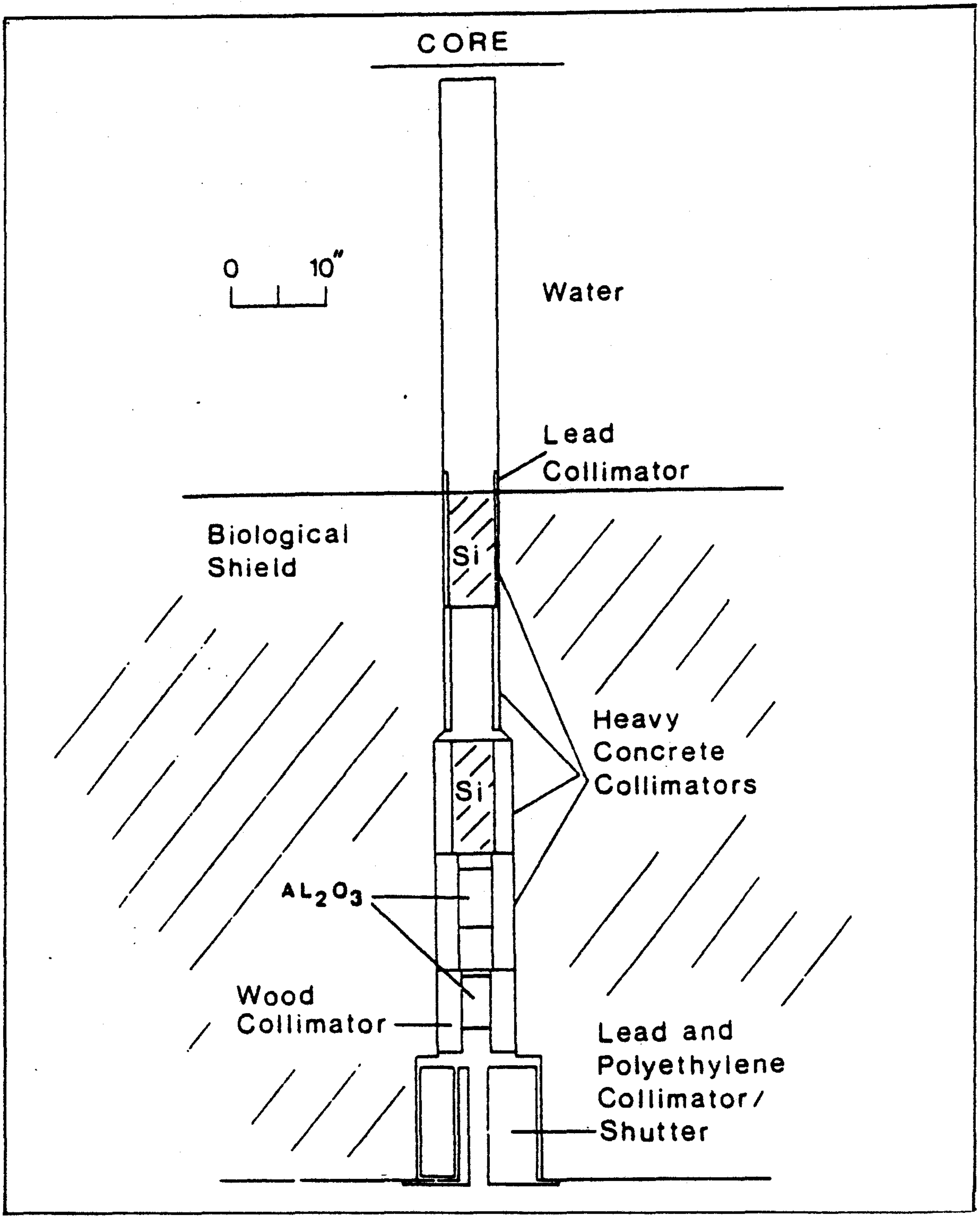
CORE
0
10"
Water
Lead
Collimator
Biological
Shield
Si
Si
Heavy
Concrete
Collimators
AL_2O_3
Wood
Collimator
Lead and
Polyethylene
Collimator/
Shutter

Figure 3.2 The neutron beam enters the "cave" at the top of the diagram. Shielding materials are lead (L), wax (W), boraflex (B), $^{6}LiCO_3$ in wax (Li) and concrete (C) (after Higgins <u>et al</u>., 1984).

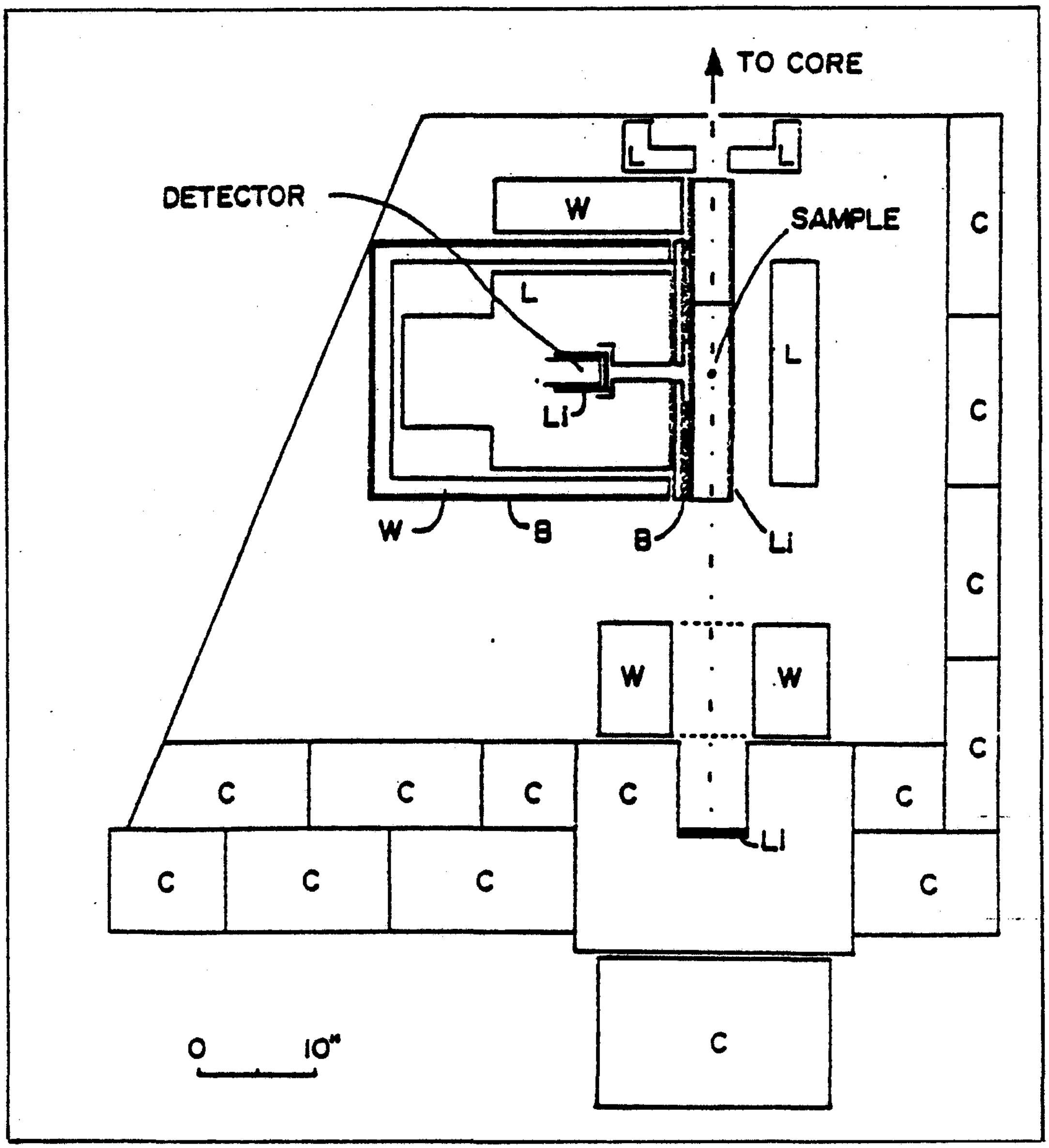
TO CORE
L
L
DETECTOR
W
SAMPLE
C
L
L
Li
C
W
B
B
Li
C
W
W
C
C
C
C
C
C
Li
C
C
C
C
C
0
10"

(1) NBS-1571 (U.S. National Bureau of Standards - Orchard Leaves)

This standard is reported to contain 33 ppm of boron.

(2) Boric acid #B-7 (McMaster University Standard)

This standard was prepared by T.A. Middleton and is reported to contain precisely 102 ug of boron. Fisher reagent grade $H_2SiO_3 \cdot nH_2O$ was used to form a matrix. Then, a 1020 ppm boron solution was made by dissolving "Specpure" boric acid in deionized, distilled water. A small amount (< 1 mL) of distilled 16 molar nitric acid was also added to this solution. Using an Eppendorf pipette, 0.102 g of solution was deposited directly onto the $H_2SiO_3 \cdot nH_2O$ matrix previously loaded into teflon tubes capped with polyethylene.

3.1.5 Precision

In order to determine the precision of the analytical procedure a rock powder with a mid-range boron content was used. An aliquot of powder R78 was irradiated three times in succession followed by the irradiation of a second aliquot, R78(P1), three times in succession, each of the six for 1000 s. Results are presented in Table 3.1 and

Table 3.1 Boron analyses for two aliquots of powder R78. The data indicates the precision of the PGNAA method

SAMPLE	IRRADIATION	BORON (ppm)	$\bar{x}$ (ppm)	σ
	1. 1000 s	5.46		
R78	2. 1000 s	5.88	5.66	0.174
	3. 1000 s	5.65		
	1. 1000 s	5.92		
R78(P1)	2. 1000 s	5.94	6.01	0.108
	3. 1000 s	6.16		

Note: The data in Table 1 were obtained using the improved mount (see text) referencing the B-7 standard.

$$\sigma = \sqrt{\frac{\Sigma x^2 - n\bar{x}^2}{n}}$$

it can be seen that the reproducibility is within experimental error. During the course of the experiments the sample mount was slightly modified to ensure that the sample was well positioned in the neutron beam thus increasing the accuracy and precision of the method. Unfortunately, due to time limitation, it was not possible to re-analyse all of the samples. Data obtained using each mount are indicated in Table 3.1 and subsequent tables.

A second precision experiment was also performed in an attempt to study the effect of sample variation. Three aliquots of a sample (i.e. R78, R78(P1), R78(P2)) were irradiated once for 1000 s each, followed by the irradiation of three aliquots of a second sample (i.e. R105, R105(P1), R105(P2)) for 1000 s each. The results are presented in Table 3.2 and show that when sample variation is considered, the reproducibility of boron concentration is still within experimental error.

3.1.6 Accuracy

In order to determine the accuracy of the system, a compound of known boron content was analysed in an attempt to reproduce this value. NBS-1571 is known to have 33 ppm of boron. An aliquot was irradiated on three separate occasions in an attempt to reproduce the accepted boron concentration. The results are shown in Table 3.3 and it

Table 3.2 Boron analyses for three aliquots of powder R78 and three aliquots of powder R105. The data indicates the precision of PGNAA when sample variation is considered

SAMPLE	IRRADIATION	BORON (ppm)	$\bar{x}$ (ppm)	σ
R78	1000 s	6.37	6.35	0.270
R78(P1)	1000 s	6.01		
R78(P2)	1000 s	6.67		
R105	1000 s	6.79	6.25	0.524
R105(P1)	1000 s	6.41		
R105(P2)	1000 s	5.54		

Note: The data in Table 2 were obtained using the original mount (see text) referencing the B-7 standard.

$$\sigma = \sqrt{\frac{\Sigma x^2 - n\bar{x}^2}{n}}$$

Table 3.3 Boron analysis of NBS-1571 (accepted B concentration = 33 ppm) referencing the B-7 standard

SAMPLE	IRRADIATION	BORON (ppm)	$\bar{x}$ (ppm)	σ	33ppm-$\bar{x}$
NBS-1571*	1. 1000 s	31.6	32.9	0.976	0.131
	2. 1000 s	33.0			
	3. 1000 s	34.0			

Note: *U.S. Bureau of Standards

The data in Table 3 were obtained using the improved mount (see text).

$$\sigma = \sqrt{\frac{\Sigma x^2 - n\bar{x}^2}{n}}$$

can be seen that the accuracy of the method is within experimental error.

3.1.7 Blank

In order to accurately determine low boron concentrations (as in most natural environments), the blank of the analytical system needed to be measured. This simply requires the irradiation (PGNAA) of an empty teflon capsule, recording the emitted boron gamma-ray energy. According to Higgins et al. (1984), the blank of the system originates from three possible sources:

(1) boron-bearing components within the detector
(2) sample packaging material
(3) scattered boron radiation from nearby boron insulation.

The blank is typically 1.4 ug of B (0.7 ppm) in a 2 gram sample (Higgins et al., 1984).

Blank data were collected on the same day as every powder analysis to ensure that each received the same neutron flux.

3.1.8 Sample Analysis

The samples (teflon capsule + polyethylene disks + rock powder) were attached to a teflon rod and lowered into the neutron beam. Most of the samples were irradiated for

1000 s but some samples required 1800 s to give a more informative gamma-spectrum. Data were collected via a Canberra Series - 85 multi-channel analyser and are presented in Table 3.4.

3.1.9 Interferences

The major problem with PGNAA as an analytical method is the interference between the various gamma-peaks which emanate from the sample. Since this experiment deals with complex natural compounds, interferences cannot be avoided. Reactions for even a single nuclide may result in a complex energy spectrum which may be further complicated by high backgrounds from other sources (Peisach, 1981a, pg. 96). This is espeically the case for (n,γ) reactions where reaction probability is high for all nuclides in the sample.

There is only one gamma-peak for boron and it lies at an energy of 478 keV. The boron peak may receive minor interference from H, Cl, Cd, P and Gd however the only important interference of the boron peak in common rocks is the Na peak at 472 keV. Na is a major constituent of most rocks; hence this interference is almost always present and must be corrected. There are several approaches to this problem but the method that has been utilized in this experiment is that devised by Higgins _et al_. (1984). The boron data were collected from the flat portion of the

Table 3.4 Boron and lithium analyses for the Mamainse Point mafic lavas (lithium analyses from Massey, 1980).

SAMPLE	IRRADIATION	BORON (ppm)	$\bar{x}$(ppm)	σ	Lithium (ppm)
R105	1. 1000 s	7.21 *	6.88	0.308	44.00
	2. 1000 s	7.26			
	3. 1800 s	6.63			
	4. 1000 s	6.49			
	5. 1000 s	6.79			
R19	1. 1800 s	4.21			16.00
R28	1. 1800 s	9.30 *	9.67	0.368	48.00
	2. 1000 s	10.0			
R63	1. 1000 s	5.79 *	6.34	0.547	26.00
	2. 1000 s	6.89			
R78	1. 1000 s	6.08 *	6.04	0.377	21.00
	2. 1000 s	6.53 *			
	3. 1000 s	6.37 +			
	4. 1000 s	5.46			
	5. 1000 s	5.88			
	6. 1000 s	5.65			
R93	1. 1000 s	6.08 *	7.01	0.926	16.00
	2. 1000 s	7.93			
R92	1. 1000 s	5.73 *	4.94	0.566	6.00
	2. 1000 s	4.60			
	3. 1000 s	4.47			
R95	1. 1000 s	10.7 *	10.1	0.575	22.00
	2. 1000 s	9.5			
R18	1. 1000 s	15.5 *			25.00

Note: *values were obtained using the original mount (see text) with reference to the NBS-1571 standard.
+values were obtained using the original mount with reference to the B-7 standard.
Values which are not marked were obtained using the improved mount (see text) with reference to the B-7 standard.

$$\sigma = \sqrt{\frac{\Sigma x^2 - n\bar{x}^2}{n}}$$

Figure 3.3 The double prompt-gamma peak of sodium and boron (after Higgins _et_ _al_., 1984).

Note: The data for the boron used in this project were collected from the flat portion of the boron peak between points A and B. This corresponds to 8 keV or 8 channels on the analyser.

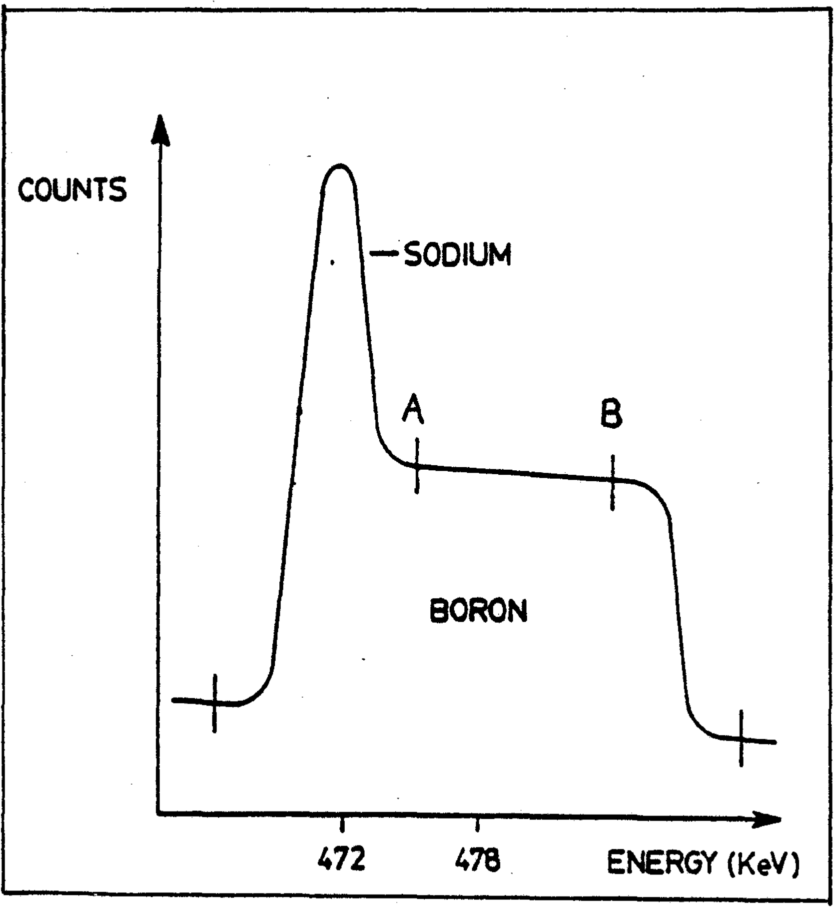
COUNTS
SODIUM
A
B
BORON
472
478
ENERGY (KeV)

Döppler broadened peak away from the Na interference peak. The boron peak with the Na interference peak is shown in Figure 3.3.

3.2 ALPHA-TRACK IMAGING

3.2.1 Introduction

An alpha map of alpha-emitting nuclides can be determined by mounting a thin section in contact with a suitable film detector and irradiating it in a full neutron flux. Heavy alpha-particles produced from a (n,α) reactions impact on CN (cellulose nitrate) film producing conical indentations of approximately 1 u in depth. These indentations may be enhanced through etching, giving a visible image.

Lithium and boron are the two elements that give the strongest alpha-track images due to the large cross sections of their (n,α) reactions. The two reactions are:

(1) $^{10}B(n,\alpha)^{7}Li$ (3840 barns)

(2) $^{6}Li(n,\alpha)^{3}H$ (945 barns).

The prompt-alpha energies for these reactions are 1.47 Mev and 2.04 Mev, respectively. These are both within the detectable limits of Kodak CN-85 film which is used for this experiment. For equal masses and normal isotopic proportions, boron gives about 13x more tracks than lithium.

When negative photographs are produced the strongest alpha-track images appear black while the weakest images appear white. A range of intensity can be observed between these extremes representing various compounds in a typical rock sample. Negative photographs of the alpha-track images for the rock samples studied are presented in Chapter 4.

Other alpha-sources include ^{14}N, ^{18}O, Fe and S but these have relatively low cross-section and can be ignored for the purposes of this experiment. Noteworthy is the fact that ^{14}N may create stray tracks as mentioned however, CN-film doped with ^{15}N has been reported to minimize this effect (M. Truscott, pers. commun.).

3.2.2 Procedure

Each thin section was placed in contact with a piece of Kodak CN-85 film. The film was then covered with a piece of polyethylene for protection purposes and to help absorb stray alpha-particles. A stack of four slides was constructed to form a "glass sandwich" (Fig. 3.4). The glass sandwich was then wrapped in polyethylene and secured with Scotch tape.

No more than four slides were irradiated at a time for reasons of practicality and absorbtion. The minerals in the thin section absorb neutrons; hence too many slides in the bundle would affect image clarity. Four slides have been

Figure 3.4 "Glass Sandwich". The diagram shows the stacking sequence used to construct the thin section bundles which were irradiated adjacent to the core of the reactor in the production of α-track images.

Note: Layers 1, 2 and 3 are in repetitive sequence whereas 4 is inverted such that glass forms the outer margins of the bundle.

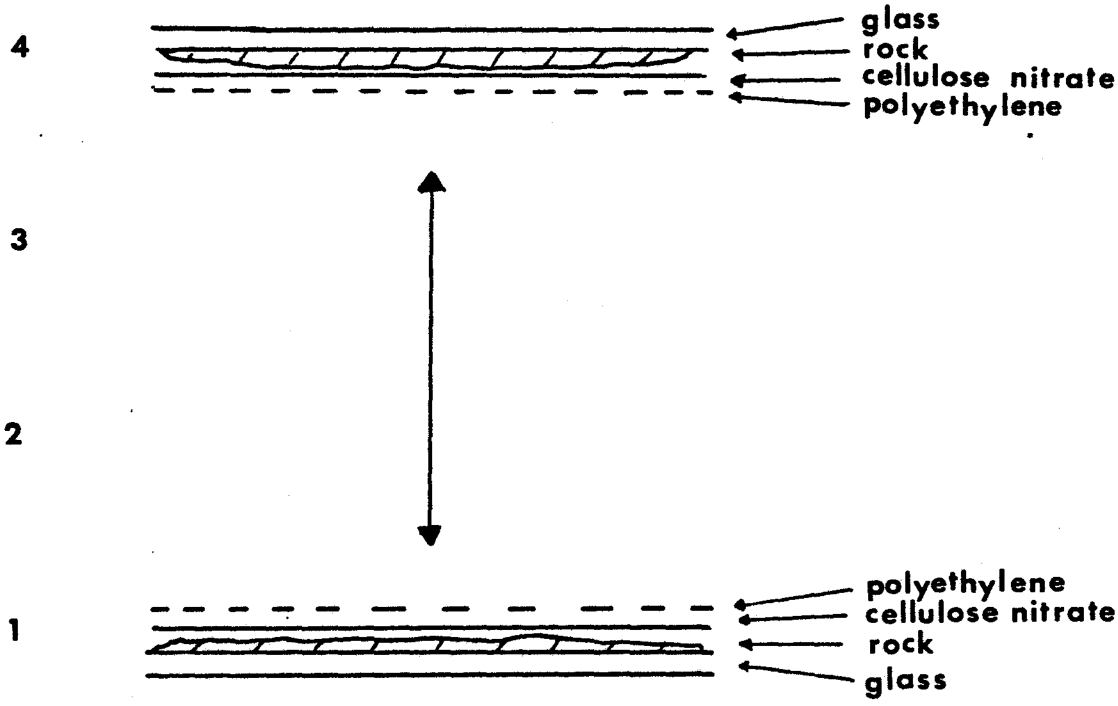
4
3
2
1
glass
rock
cellulose nitrate
polyethylene
polyethylene
cellulose nitrate
rock
glass

found to be better than six, and so on (M. Truscott, pers. commun.).

Each bundle was irradiated for twelve minutes adjacent to the core of the McMaster University reactor after which they were allowed to cool for one week.

An etching solution consisting of 25 g NaOH in 250 mL distilled water (2.5 N) was made and then heated to a temperature of 50°C. The CN-film was carefully separated from the thin section and then was suspended (using aligator-clips) in the etching solution for approximately fifteen minutes. The film was then promptly removed from the solution, rinsed with distilled, deionized water to ensure the termination of the etching process and dried.

The alpha-track images were then mounted and photographed. These are shown alongside photographs of the thin sections in Chapter 4.

CHAPTER 4

COMPARISON OF THE PETROGRAPHY AND THE ALPHA-TRACK IMAGES FOR THE MAMAINSE POINT MAFIC VOLCANICS

4.1 INTRODUCTION

The primary mineralogy of the mafic lavas consists of plagioclase (An_{55-60}), clinopyroxene (mostly augite variety) and iron-oxides (magnetite oxidized to hematite). No fresh olivine was observed in any of the specimens. Varying proportions of glass also occur throughout the rock.

The dykes have a primary mineralogy of plagioclase, clinopyroxene and opaque iron-oxides.

The Mamainse Point Formation has suffered low grade burial metamorphism in the zeolite and prehnite-pumpellyite facies regime. As a result, the primary mineralogy has been degraded and new mineral phases have been developed. These are best observed in amygdules throughout the rock. Since the metamorphism is only low grade, the primary textures of the rock have been retained.

Secondary mineral phases include: albite, chlorite, calcite, quartz, stilpnomelane, chalcedony, epidote, prehnite, pumpellyite, iron oxide, and laumontite.

The mineralogy of the Mamainse Point area has been previously studied by Annells (1973) and Massey (1980).

The objective of this chapter is to qualitatively associate the rock mineralogy to the B(Li) concentrations observed through alpha-track imaging. The discussion will commence at the bottom of the stratigraphic column, namely the Alona Bay flows and proceed systematically through the Mamainse Point Series as defined by Massey (1980) including the Daisy Stone Flow and the dykes.

Photographs of the thin sections and the alpha-track images for each of the rocks have been prepared and will be presented side by side for comparative purposes.

4.2 PETROGRAPHY AND ALPHA-TRACK IMAGING

4.2.1 The Alona Bay Flow (R105)

The primary mineralogy of this specimen consists of plagioclase, clinopyroxene and opaque, iron-oxides (Plate 1a, site 1). The plagioclase occurs in phenocrysts up to 2 mm which have been altered to albite, chlorite and epidote (Plate 1a, site 2). Clinopyroxene occurs mostly in aggregates of subhedral crystals throughout the rock. Individual grains are up to 0.4 mm. Plagioclase, clinopyroxene, opaque grains (up to 0.2 mm), glass and

Plate 1. Sample R105: 1a, thin section; 1b, ATI; scale bar 5 mm.

B = 6.88 ppm (Table 3.4)

Li = 44.00 ppm

Site 1. A group of iron oxide grains (magnetite partially oxidized to hematite) are to the left of the marker. On the ATI they are seen to be the source of strong B(Li) images.

Site 2. A plagioclase phenocryst surrounds a chlorite-rich area and iron-oxide inclusions, just to the left of the marker. The α-track images are strong from the chlorite and the iron-oxides, but very weak from the plagioclase.

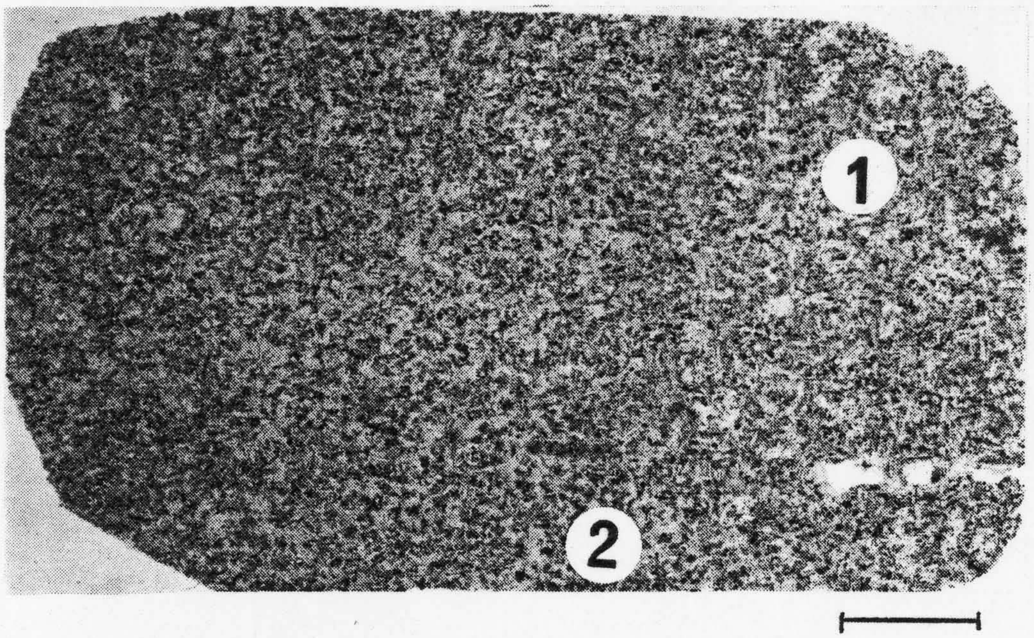

Plate]a

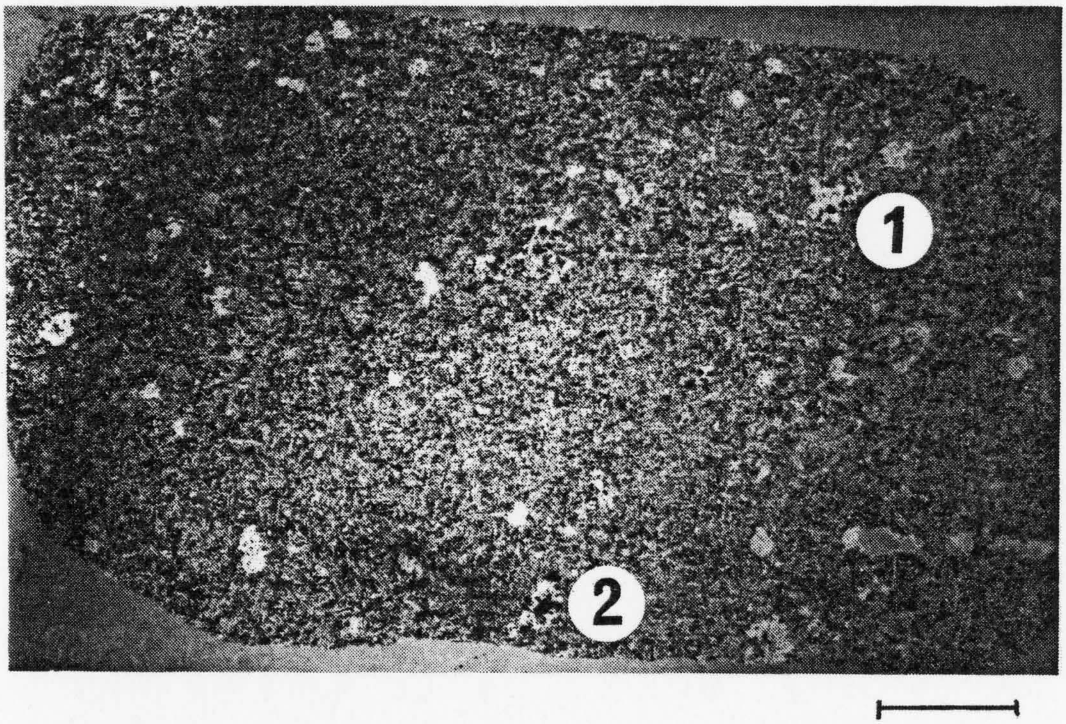

Plate]b

chlorite occur interstitially between the larger plagioclase phenocrysts and clinopyroxene aggregates. Some of the opaque grains are intimately associated with iddingsite which may represent an alteration product of olivine. Many amygdules filled with light green chlorite (anomalous steely blue birefringence) are common in the rock.

This specimen is medium-grained and possesses a gabbroic texture, that is, "a coarse-grained holocrystalline rock with placioclase laths, subhedral pyroxene, and magnetite" (Massey, 1980).

Modal abundances of minerals were estimated visually and are presented in the table below. Visual estimations of mineral abundances were performed for each specimen and the error in the estimates, for the major phases, is approximately ±5%.

	Mineral	Abundance
Primary:	Plagioclase	40%
	Clinopyroxene	30%
	Opaques (Fe-oxide)	10%
	Glass	2%
Secondary:	Albite	5%
	Epidote	2%
	Chlorite	8%
	Iddingsite	3%

4.2.2 Series I (R19)

This rock consists of stilpnomelane pseudomorphs of olivine up to 4 mm in size (Plate 2a, sites 1, 2, 3) set in

Plate 2. Sample R19: 2a, thin section; 2b, ATI; scale bar 5 mm.

B = 4.21 ppm (Table 3.4)

Li = 16.00 ppm

Site 1. A cluster of stilpnomelane grains showing opaque iron-oxide rims can be seen to the left of the marker. Iron-oxide also fills fractures within the grains. The α-track images are strong from the opaque rims and fracture fills and medium from the stilpnomelane grains themselves.

Site 2. A rectangular stilpnomelane grain with an opaque iron-oxide rim is to the left of the marker. On the ATI the rim gives a strong track image and the stilnomelane gives a medium image.

Site 3. A large stilpnomelane grain with opaque iron-oxide fracture fillings and rim can be seen just to the left of the marker. On the ATI the rim and fractures give strong track images while the stilpnomelane gives a medium image.

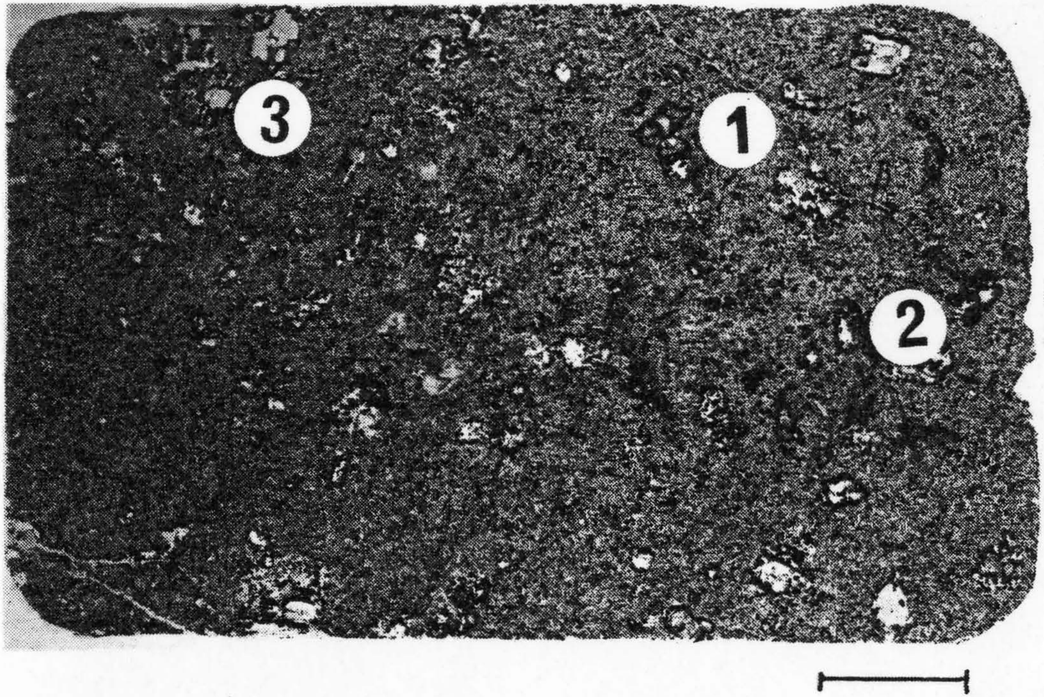

Plate 2a

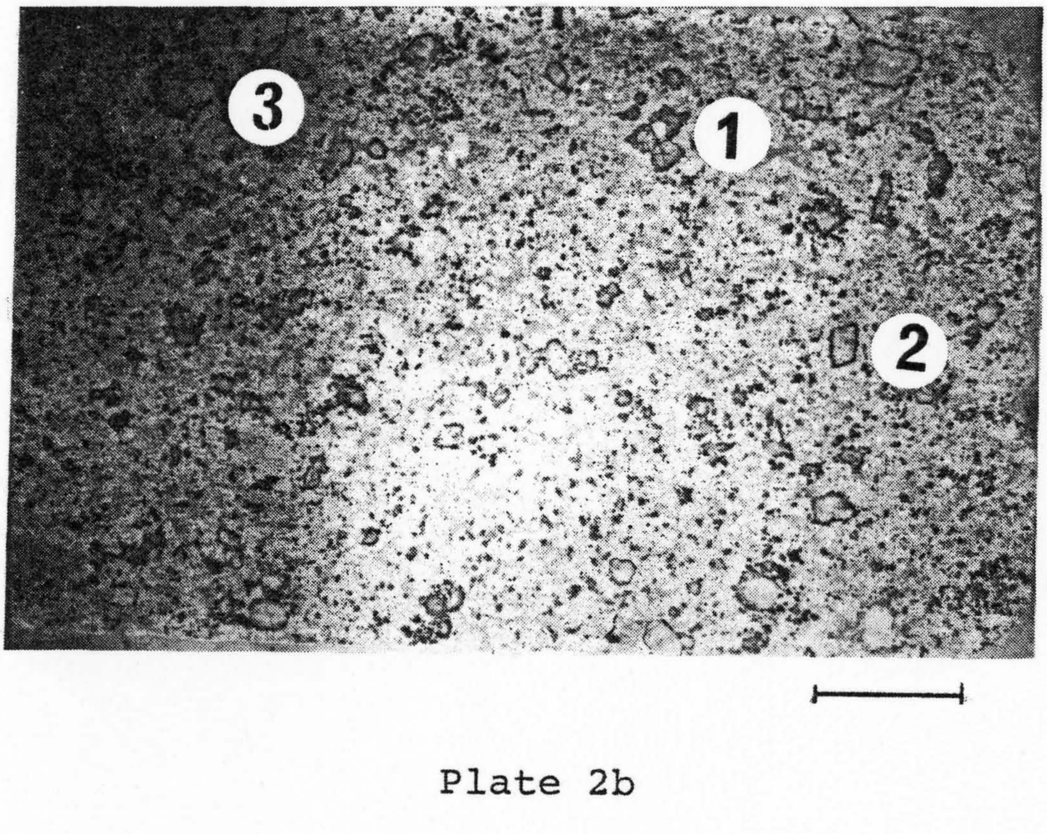

Plate 2b

a fine-grained matrix of fairly fresh plagioclase laths up to 0.4 mm, granular clinopyroxene up to 0.4 mm, opaque iron-oxides up to 0.7 mm and glass ± chlorite. The stilpnomelane shows brownish-yellow to green pleochroism, moderate relief with n > balsam, parallel extinction and a uniaxial negative interference figure.

The clinopyroxene occurs in twinned phenocrysts up to 1.25 mm throughout the rock. Opaque minerals occur as grains within the groundmass or in rims and/or fractures associated with the stilpnomelane phenocrysts. The plagioclase laths can often be seen in radiating clusters with interstial clinopyroxene and opaques. The matrix consists of clinopyroxene and opaques and is interstitial to the phenocrysts giving the rock a porphyritic texture.

The modal abundances of the minerals in this sample are given below.

	Mineral	Abundance
Primary:	Plagioclase	31%
	Clinopyroxene	26%
	Opaques (Fe-oxide)	15%
	Glass	1%
Secondary:	Chlorite	5%
	Stilpnomelane	22%

Overall the alpha-track image for this rock (Plate 2b) shows three levels of intensity: a low intensity corresponding to the groundmass; a medium intensity corresponding to the stilpnomelane pseudomorphs; and, finally, a high intensity corresponding to the rims encompassing the stilpnomelane pseudomorphs and opaque inclusions and fracture fills within the stilpnomelane. The low intensity images result from areas which are poor in B(Li) while high intensity images result from areas rich in B(Li). Stilpnomelane psuedomorphs with opaque rims are shown in Plate 2b, sites 1, 2, and 3.

4.2.3 The Daisy Stone Flow (R18)

This rock is very coarse-grained and one immediately notices its spectacular glomerophitic texture. Plagioclase occurs in laths up to 15 mm which are highly fractured and altered to albite, pumpellyite, epidote and prehnite. Clinopyroxene is also present in the rock and occurs in grains up to 5.5 mm in size. It often forms optically continuous networks around radiating plagioclase laths to give the rock its primary glomerophitic texture. A small amount of olivine can be seen in the rock but it is highly fractured and mineralized by opaque phases.

Chlorite occurs throughout the rock in three modes of occurrence. Chlorite (a) is light green in colour and psosesses a steely blue birefringence. It occurs in amygdules throughout the rock or as a pseudomorph of olivine. In the latter case opaque minerals and iddingsite often fill fractures within the grains, and opaques often form rims. Chlorite (b) (Plate 3a, site 1) is dark green in colour and has a low birefringence. It may have some glass associated with it. Chlorite (b) can be observed throughout the slide but is most prominent in halos encompassing amygdules as shown in Plate 3a. Finally, chlorite (c), a light greenish-yellow coloured mineral with high (2nd order) birefringence, was observed. This type of chlorite was common in amygdules throughout the rock (Plate 3a, site 3).

Most of the iron-oxides occur in anhedral to subhedral grains up to 0.75 mm in size and are for the most part magnetite oxidized to hematite. As previously mentioned, the opaques may be intimately associated with iddingsite.

There are several mineralized amygdules throughout the rock containing calcite (Plate 3a, site 2) and chlorite. They may be as much as 5 mm in diameter, but the majority are only 2.5 mm across and irregular in shape.

There are also traces of pumpellyite throughout the rock being an alteration product of plagioclase.

The modal abundances of these minerals are listed below.

Plate 3. Sample R18: 3a, thin section; 3b, ATI; scale bar 5 mm.

B = 15.5 ppm (Table 3.4)

Li = 25.00 ppm

Site 1. A calcite amygdule with a rim of chlorite (c) and a halo of dark green chlorite (b) can be seen just to the left of the marker. On the ATI, the calcite gives a weak image as does the halo of chlorite (b). However chlorite (c) gives a relatively strong image indicating high B(Li) content.

Site 2. A large circular calcite amygdule can be seen to the left of the marker. It has a rim of chlorite (c). On the ATI the calcite gives a weak image while the chlorite rim gives a strong image.

Site 3. An amygdule containing chlorite (c) can be seen to the left of the marker. On the ATI, it is seen to be the source of a strong B(Li) image.

Site 4. Plate 3b only. Strong α-track images of pumpellyite grains can be seen just to the left and just below the marker.

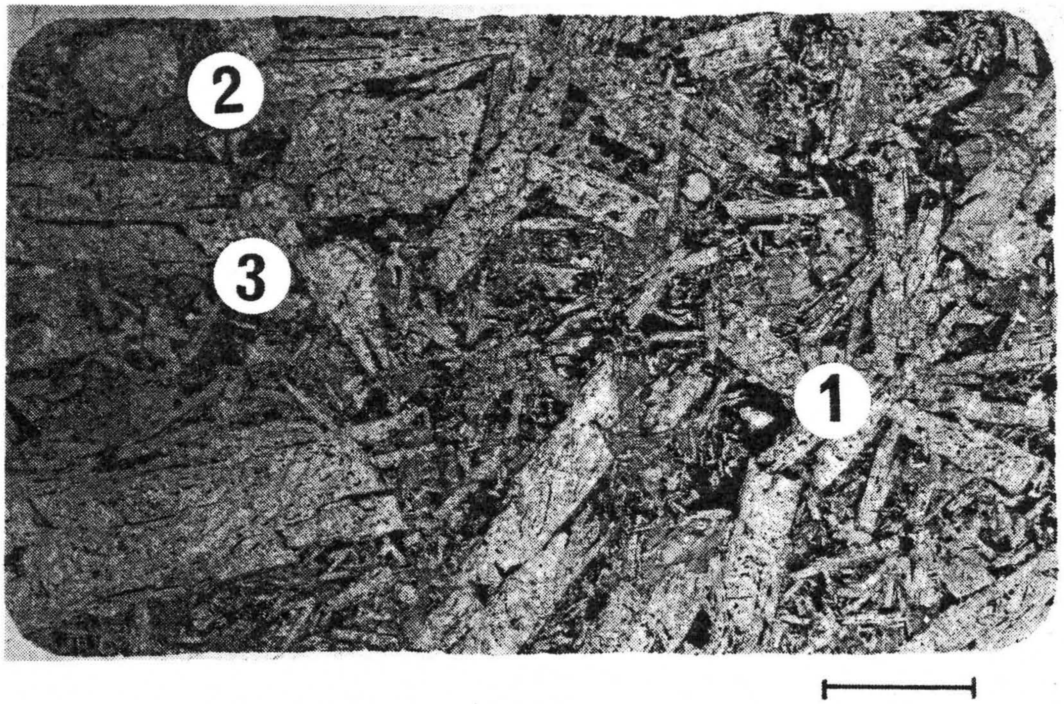

Plate 3a

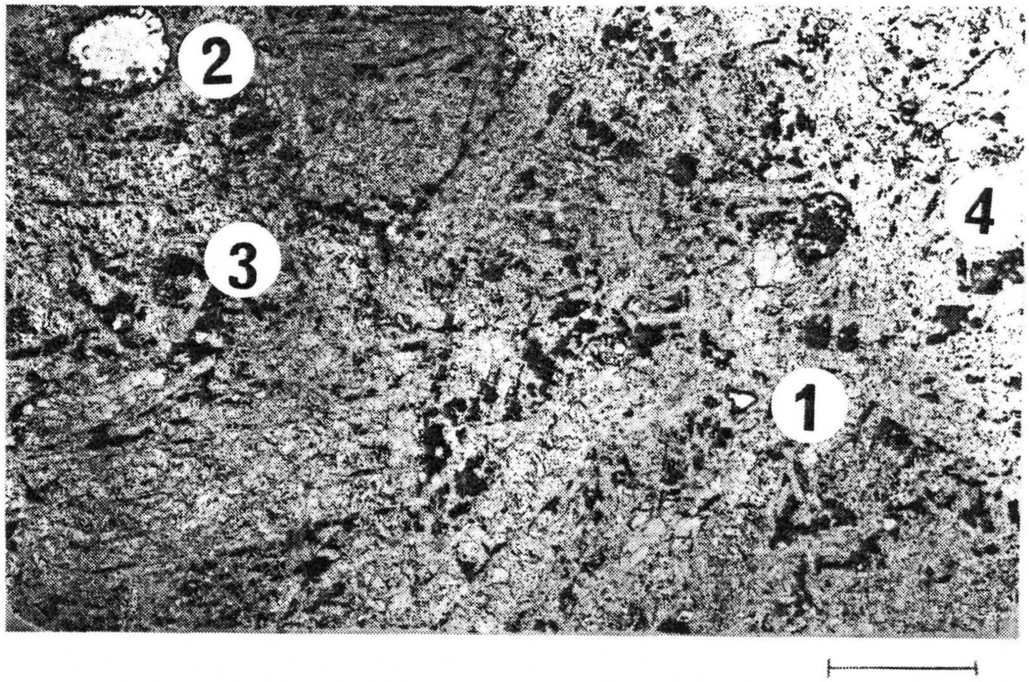

Plate 3b

	Mineral	Abundance
Primary:	Plagioclase	45%
	Clinopyroxene	15%
	Opaques (Fe-oxide)	10%
	Olivine	<1%
Secondary:	Chlorite	17%
	Calcite	5%
	Epidote	1%
	Albite	3%
	Prehnite	1%
	Pumpellyite	1%
	Iddingsite	2%

For the alpha-track image of this specimen (Plate 3b), the lowest intensity signals are given by plagioclase, clinopyrexene and calcite (Plate 3b, site 2). The most intense tracks are given by chlorite (a), chlorite (c) (Plate 3b, site 3) and the opaque minerals. Chlorite (b) gives a very weak image (Plate 3b, site 1).

Strong alpha-track images were also correlated to pumpellyite grains (Plate 3b, site 4) and to point concentrations in plagioclase (prehnite and pumpellyite alteration?).

4.2.4 Series II (R28)

This rock is composed of plagioclase laths up to 2 mm in size, clinopyroxene grains up to 0.6 mm and opaque iron-oxides up to 2 mm. Much of the plagioclase has been altered to albite and a radiating colourless mineral possessing high birefringence (prehnite?) which is very fine-grained (Plate 4a, site 1). There is some iddingsite

Plate 4. Sample R28: 4a, thin section; 4b, ATI; scale bar 5 mm.

B = 9.67 ppm (Table 3.4)

Li = 48.00 ppm

Site 1. A cluster of plagioclase phenocrysts with albite and prehnite(?) alteration can be seen to the left of the marker. On the ATI, the cluster gives a weak track image indicating low B(Li) content.

Site 2. A group of iron-oxide grains (magnetite partially oxidized to hematite) with a small amount of intergrown iddingsite can be seen to the left of the marker. The ATI indicates them to be a source of strong B(Li) images.

Site 3. A small elongate amygdule containing chlorite and chalcedony is to the left of the marker. It gives intermediate B(Li) values on the ATI.

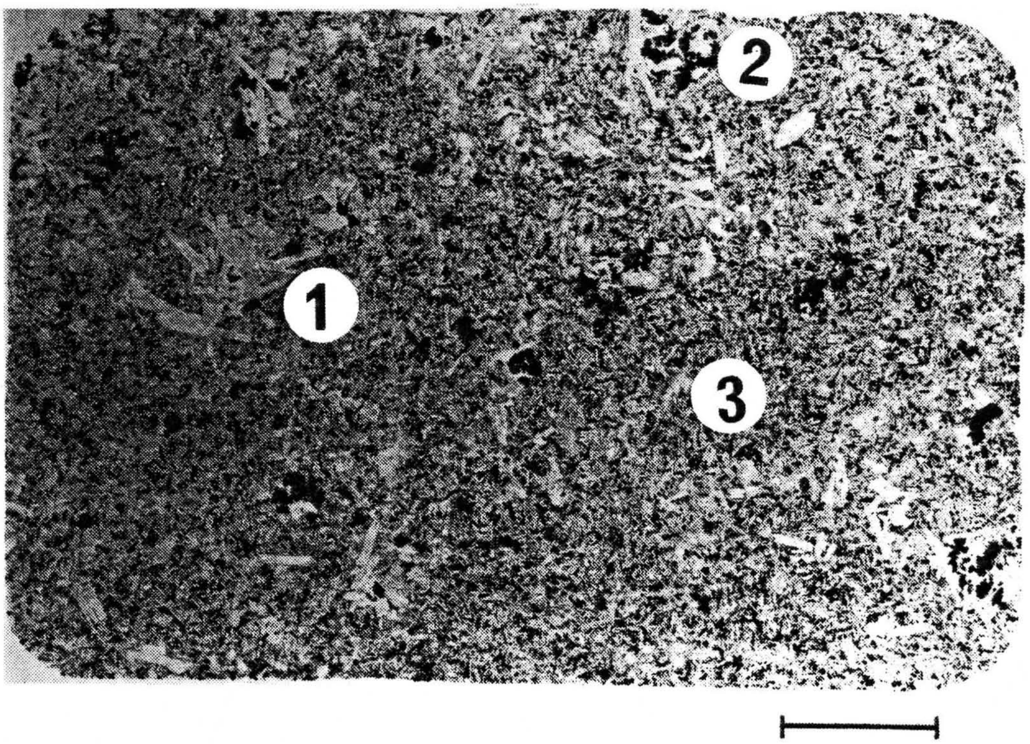

Plate 4a

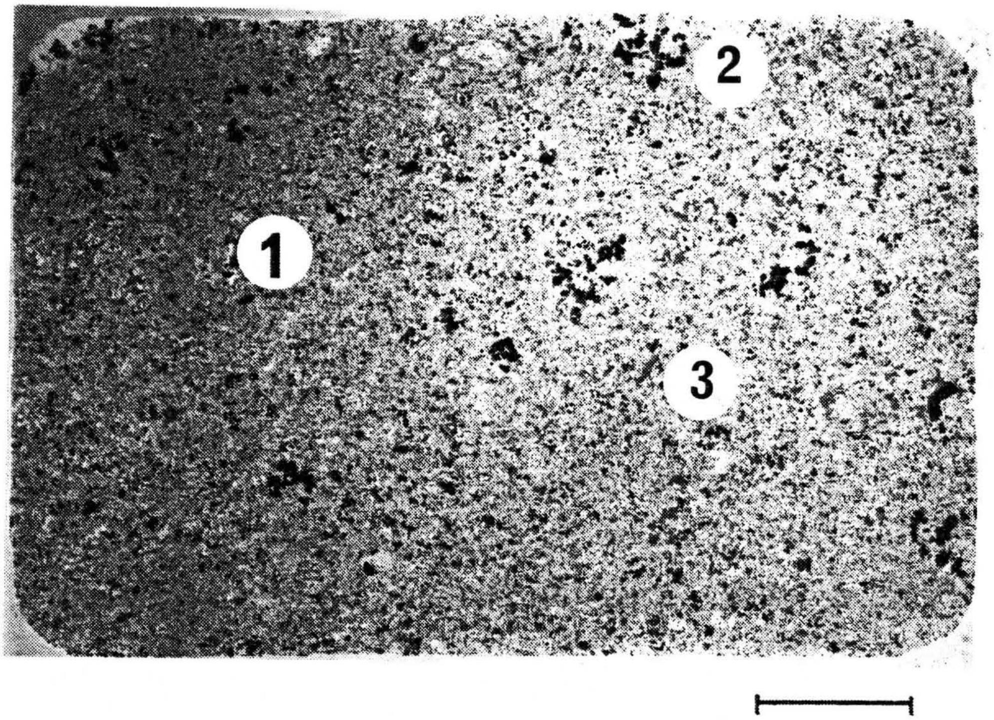

Plate 4b

pseudomorphed after olivine in the sample which occurs in 0.2 mm grains, however iron-oxides have formed in the fractures of many of the iddingsite crystals as well as in rims surrounding them. The iron-oxides dominate volumetrically over the iddingstite phase to a point where very little iddingsite remains in some aggregates (Plate 4a, site 2).

Chlorite and chalcedony(?) occur in amygdules throughout the rock (Plate 4a, site 3). Calcite is a minor constituent of the rock and occurs in grains up to 0.15 mm in size.

This specimen is fairly coarse grained. The plagioclase is, on occasion, found as radiating clusters with interstitial clinopyroxene and fine-grained plagioclase. Overall, the rock has a gabbroic or intergranular texture.

A modal analysis for the mineralogy of this rock is presented below.

	Mineral	Abundance
Primary:	Plagioclase	40%
	Clinopyroxene	7%
	Opaques (Fe-oxide)	3%
Secondary:	Albite	4%
	Calcite	3%
	Epidote	1%
	Chlorite	7%
	Chalcedony	3%
	Iddingsite	5%

There seems to be three distinct intensity levels on the alpha-track image for this rock (Plate 4b). There is a low intensity corresponding to plagioclase (Plate 4b, site 1) and clinopyroxene, a medium intensity corresponding to the chlorite/chalcedony amygdules (Plate 4b, site 3) and a high intensity corresponding to the opaque grains (Plate 4b, site 2). Therefore, once again it can be seen that chlorite and iron-oxides have higher proportions of B(Li) compared to other minerals in the rock. Noteworthy is that when iddingsite is associated with opaque minerals it gives an alpha-track image of comparable intensity to chlorite.

4.2.5 Series III (R63)

The primary mineralogy of this rock consists of plagioclase, clinopyroxene, opaque iron-oxides and a small amount of glass.

The plagioclase occurs in two forms:

(a) phenocrysts up to 4 mm in size,

(b) fine-grained laths in the matrix of the rock up to 0.1 mm in size.

Clinopyroxene and iron-oxides complete the matrix and occur in grains up to 0.1 mm and 0.2 mm respectively. Glass, interspersed with some chlorite, is interstitial.

The rock shows excellent primary, porphyritic texture. The plagioclase phenocrysts are usually fractured and may show occasional zonation (Plate 5a, site 1) however,

Plate 5. Sample R63: 5a, thin section; 5b, ATI; scale bar 5 mm.

B = 6.34 ppm (Table 3.4)

Li = 26.00 ppm

Site 1. A large plagioclase phenocryst to the upper left of the marker shows zonation and inclusions of iron-oxides. The ATI shows that B(Li) are concentrated along the microfractures and in the core of the plagioclase crystal.

Site 2. A euhedral opaque iron-oxide grain within a plagioclase phenocryst is to the upper left of the marker. On the ATI, the iron-oxide is seen to be a source of a strong α-track image while the plagioclase image is very weak.

Site 3. A chlorite amygdule with a chalcedony(?) rim is to the left of the marker. On the ATI the chlorite is seen to give a very strong image while the chalcedony rim gives a weak image.

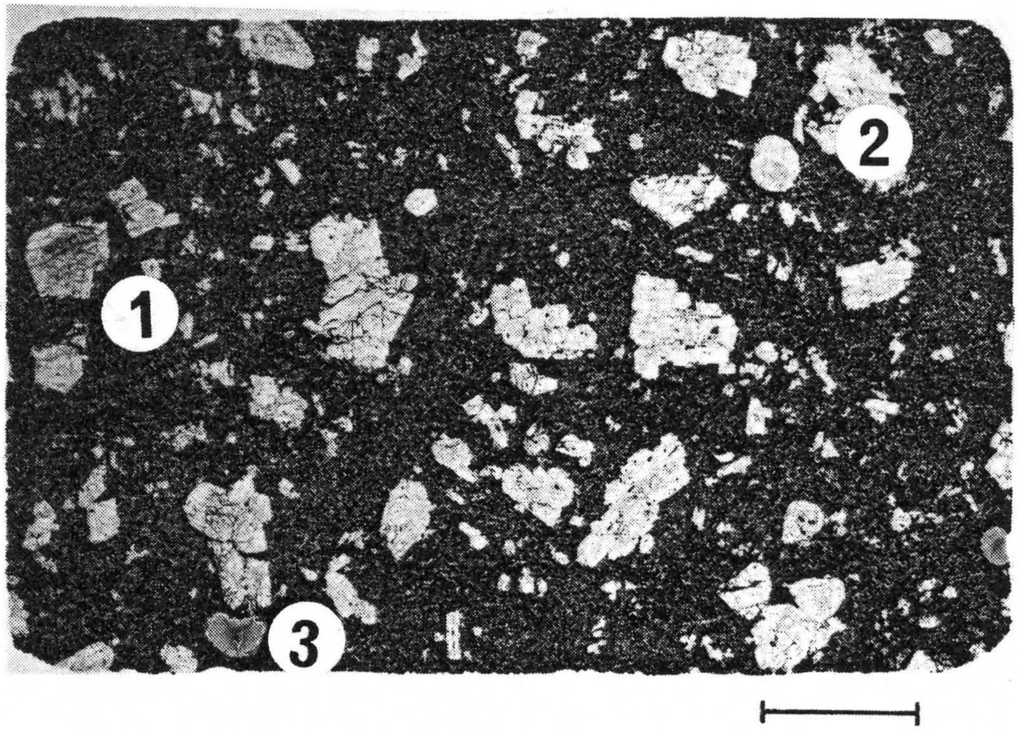

Plate 5a

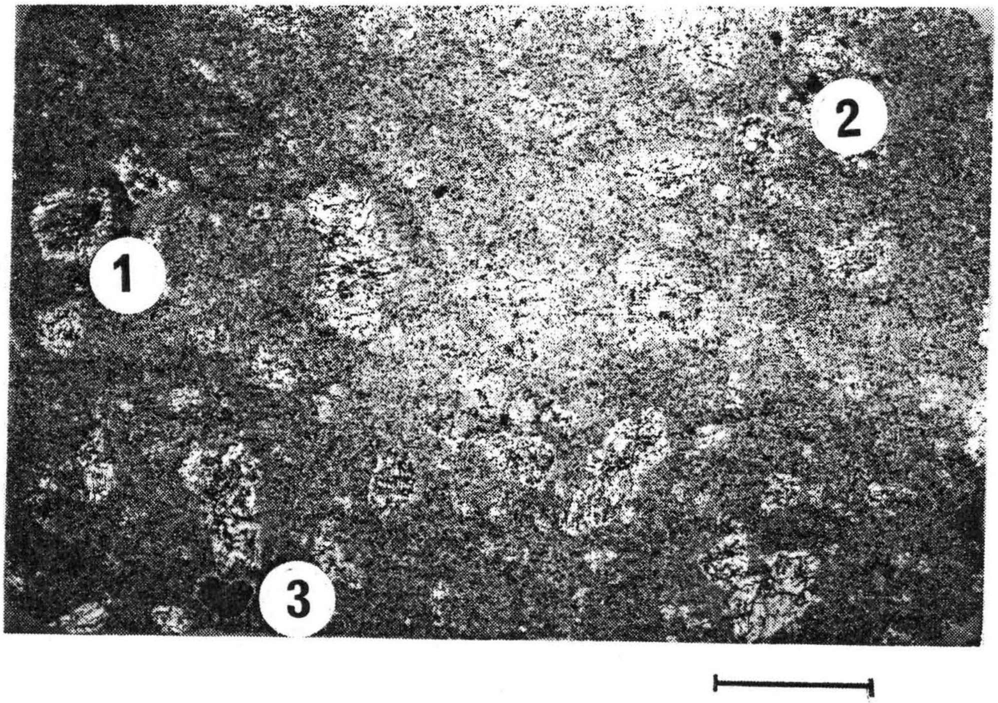

Plate 5b

they are still fairly fresh. Some of the fractures are partially mineralized by iddingsite and chlorite. Opaque inclusions also occur in the plagioclase phenocrysts. Some are euhedral (Plate 5a, site 2) but for the most part, these inclusions are fracture controlled and very fine-grained.

Chlorite also occurs in amygdules which are up to 2.3 mm across. The amygdules show rims of a fine-grained fibrous material that has low relief and low (1st order) birefringence. This is probably chalcedony (Plate 5a, site 3).

The modal analysis for the rock is shown below.

	Mineral	Abundance
Primary:	Plagioclase	55%
	Clinopyroxene	23%
	Opaques (Fe-oxide)	15%
	Glass	1%
Secondary:	Chlorite	4%
	Iddingsite	1%
	Chalcedony	1%

The strongest alpha-track images came from three sources:

(a) opaque iron-oxide grains which are somewhat reddish (hematite oxidation of magnetite?) (Plate 5b, site 2),

(b) chlorite in amygdules (Plate 5b, site 3),

(c) microfractures in plagioclase phenocrysts (Plate 5b, site 1).

The fine-grained matrix of the rock gives an alpha-track image which shows intermediate B(Li). Intense point concentrations of B(Li) in the matrix sum to correspond to fine-grained iron-oxide.

Areas of fresh plagioclase are very low in B(Li).

4.2.6 Series IV (R78)

The mineralogy of this rock consists of plagioclase laths up to 1 mm, clinopyroxene grains up to 0.8 mm and opaque iron-oxide grains up to 0.75 mm.

Many prominent grains showing a very light green pleochroism occur throughout the slide. This mineral has 1st order birefringence and is probably chlorite pseudomorphed after olivine. Opaque minerals are in intimate association with these aggregates, mostly in fractures. There is also a small amount of glass throughout the rock.

Several amygdules can be observed and these are mineralized with light emerald green chlorite and quartz (Plate 6a, site 2). The quartz occurs in rims encompassing the chlorite amygdules or as small irregular veinlets within the amygdule itself. In the latter case the quartz grains are <<0.1 mm.

There are clusters of intergrown grains of clinopyroxene and plagioclase in the rock giving rise to

Plate 6. Sample R78: 6a, thin section; 6b, ATI; scale bar 5 mm.

B = 6.00 ppm (Table 3.4)

Li = 21.00 ppm

Site 1. An aggregate of opaques, chlorite pseudomorphed after olivine and plagioclase can be seen just to the left of the marker. On the ATI the opaques give a strong image, the chlorite gives a medium image and the plagioclase gives a weak image.

Site 2. An irregular chlorite amygdule can be seen just to the left of the marker. It contains a small amount of quartz. It is seen to be the source of a medium B(Li) image on the ATI.

Site 3. Plate 6b only. Several strong α-track images of opaque grains can be seen just to the left of the marker.

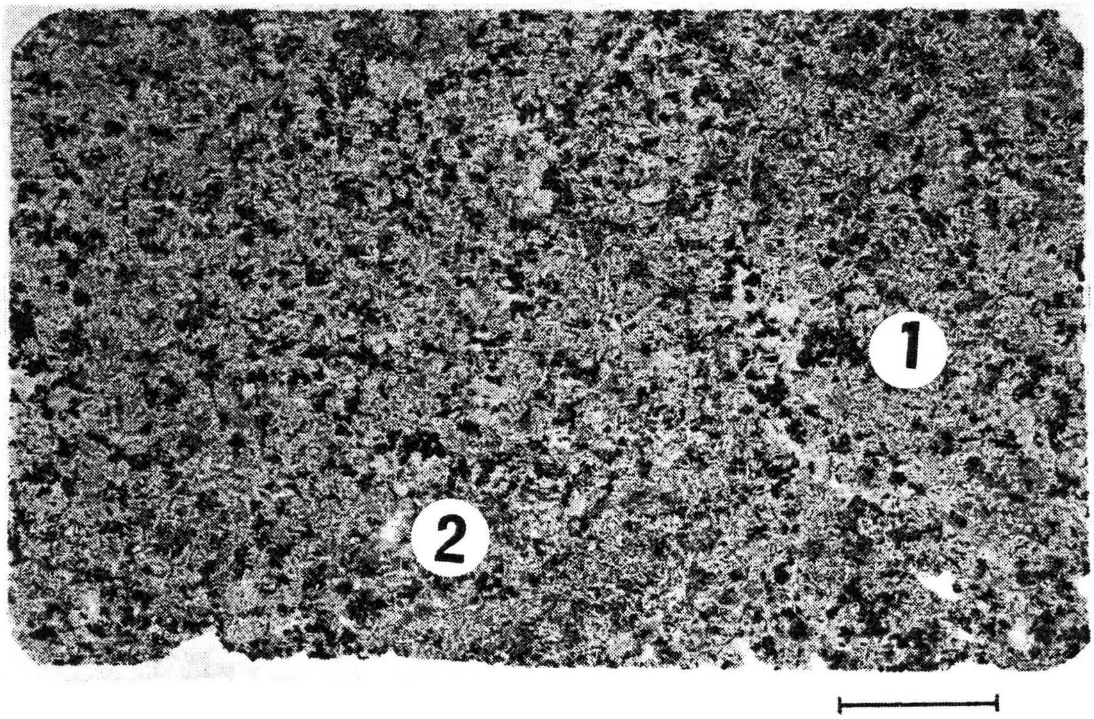

Plate 6a

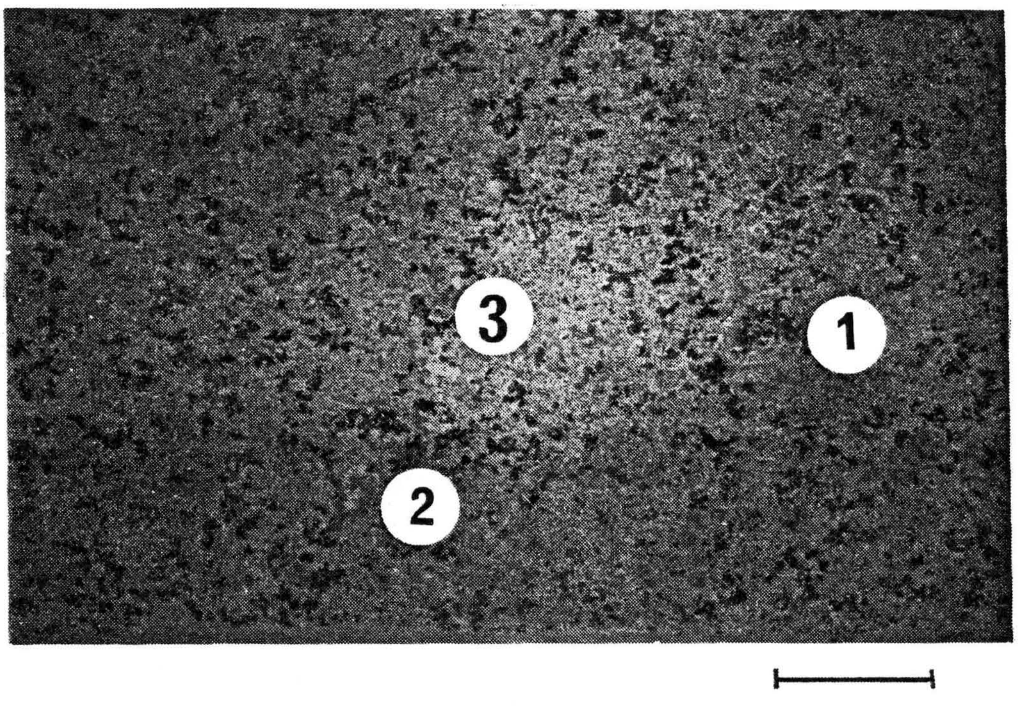

Plate 6b

ophitic or sub-ophitic textures. The clinopyroxene shows optical continuity in crossed nicols. The plagioclase may be radiating to form glomerocrysts but these are not as spectacular as in the Daisy Stone Flow.

Calcite has replaced some of the plagioclase but it can also fill cavities. The latter have quartz coronas in some cases.

The modal analysis for the rock is given below.

	Mineral	Abundance
Primary:	Plagioclase	30%
	Clinopyroxene	30%
	Opaques (Fe-oxide)	10%
	Glass	1%
Secondary:	Chlorite	22%
	Calcite	6%
	Quartz	1%

The strongest alpha-track images are produced by the opaque iron-oxides (Plate 6b, site 3). Medium intensity alpha-track images are produced by chlorite pseudomorphed after olivine (Plate 6b, site 1) and chlorite amygdules (plate 6b, site 2). Low intensity alpha-track images are derived from plagioclase and clinopyroxene.

4.2.7 Series V (R92)

The primary mineralogy of this rock consists of palgioclase laths up to 0.75 mm, clinopyroxene grains up to 1 mm and opaque iron-oxides (Plate 7a, site 1) up to 0.5 mm. Some glass also occurs interstitially throughout the rock.

Plate 7. Sample R92: 7a, thin section; 7b, ATI; scale bar 5 mm.

B = 4.94 ppm (Table 3.4)

Li = 6.00 ppm

Site 1. Several elongate opaque grains can be seen just to the left of the marker. On the ATI they are seen to be sources of weak B(Li) tracks.

Site 2. Chlorite (a) mineralization is just to the upper left of the marker. On the ATI it is seen to be the source of strong B(Li) tracks.

Site 3. A fibrous grain of a mineral that has not been positively identified (possibly prehnite, datolite or danburite) can be seen just to the left of the marker. On the ATI, this mineral is a source of strong B(Li) tracks.

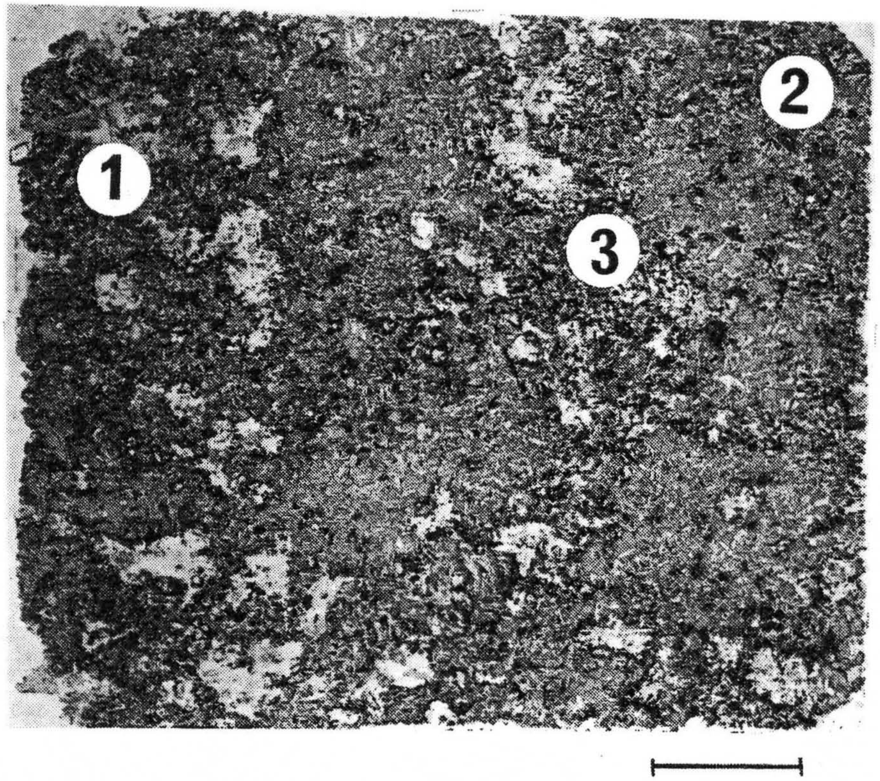

Plate 7a

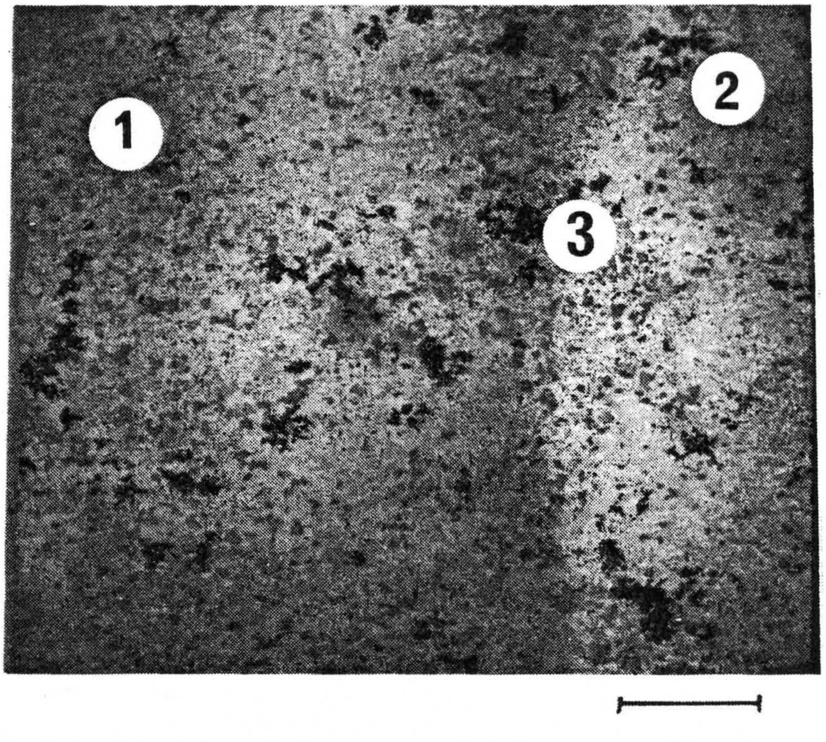

Plate 7b

Although the clinopyroxene and the plagioclase are quite fresh, there are many types of secondary minerals in this sample. The major secondary phase is stilpnomelane which occurs in isolated crystals throughout the rock. Chlorite also occurs and is found in two distinct varieties. The first type, chlorite (a), occurs as an alteration of plagioclase and may be observed on the surface of this mineral in thin section (Plate 7a, site 2). Chlorite (a) may also be found in the intersticies between primary minerals. It does not have clear interference colours and appears in light green clumps of very fine-grained crystals. The second type, chlorite (b), occurs in fan-like aggregates of needle-shaped crystals. These masses have low birefringence and show undulose extinction due to their fibrous mode of occurrence.

There is also a seocndary mineral in the rock which has not been positively identified. It occurs in fine-grained traces throughout the rock but may also form clumps up to 1.75 mm in size (Plate 7a, site 3). It has low relief (n is approximately 1.6), low birefringence (highest interference colours are first order red), length fast crystals and has a very light green colour in plain light. This mineral could be prehnite, datolite or danburite.

The rock shows prominent glomerophitic texture in which clinopyroxene may surround radiating laths of plagioclase. The clinopyroxene retains optical continuity. Where glomerocrysts are not present, clinopyroxene and plagioclase form an intergranular network with interstial chlorite ± glass.

A modal analysis for the mineralogy of this rock is given below.

	Mineral	Abundance
Primary:	Plagioclase	30%
	Clinopyroxene	26%
	Opaques (Fe-oxide)	3%
	Glass	2%
Secondary:	Stilpnomelane	15%
	Chlorite (a)	20%
	Chlorite (b)	3%
	Unknown mineral	1%

The alpha-track image for this rock (Plate 7b) reveals that B(Li) is concentrated in discrete packages throughout the rock. The most intense B(Li) tracks are produced by chlorite (a) and the unknown fibrous mineral (Plate 7b, sites 2 and 3 respectively). Medium intensity tracks can be correlated to the stilpnomelane grains while the lowest intensity tracks correspond to chlorite (b), plagioclase, clinopyroxene and the opaque grains (Plate 7b, site 1).

4.2.8 Series V (R93)

The primary constituents of this rock are plagioclase laths up to 2.25 mm, clinopyroxene grains up to

1.2 mm and opaque iron-oxides up to 1 mm (Plate 8a, site 1).

Amygdules up to 5.5 mm in diameter are filled with calcite, chlorite and devitrified glass. Some of the amygdules have rims consisting of chalcedony and chlorite ± glass (Plate 8a, site 2). Small veinlets of granular quartz (<<1 mm) also occur within the amygdules. Chlorite mineralization interwoven with iron-oxides also occurs in the intersticies of plagioclase and clinopyroxene.

Clinopyroxene is interstitial to plagioclase forming ophitic to sub-ophitic texture. Interstitial glass is also present throughout the rock.

Some of the opaque grains in the rock are intergrown with iddingsite suggesting derivation from pre-existing olivine.

A modal analysis for the mineralogy of this rock is presented below.

	Mineral	Abundance
Primary:	Plagioclase	43%
	Pyroxene	20%
	Opaques (Fe-oxide)	13%
	Glass	5%
Secondary:	Calcite	3%
	Chlorite	12%
	Quartz	1%
	Iddingsite	2%
	Chalcedony	1%

The strongest alpha-track images are produced by the opaque minerals (Plate 8b, site 1). The interwoven chlorite and iron-oxide have an intermediate concentration of B(Li)

Plate 8. Sample R93: 8a, thin section; 8b, ATI; scale bar 5 mm.

B = 7.01 ppm (Table 3.4)

Li = 16.00 ppm

Site 1. Several opaque grains can be seen to the upper left of the marker. The ATI shows that they are a strong source of B(Li) tracks.

Site 2. A large amygdule containing calcite and chlorite can be seen to the left of the marker. The structure possesses a rim of chalcedony and chlorite ± some glass. On the ATI, the contents of the amygdule show low B(Li) concentration, however the chlorite in the rim of the amygdule is a strong source of B(Li) tracks.

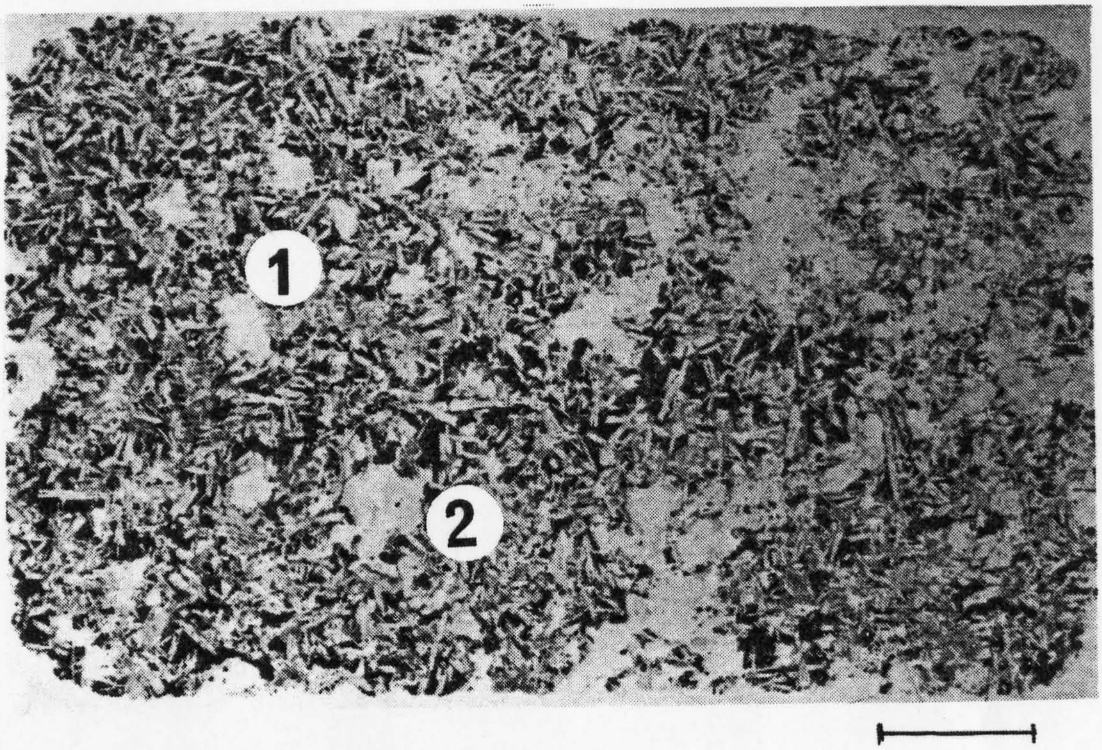

Plate 8a

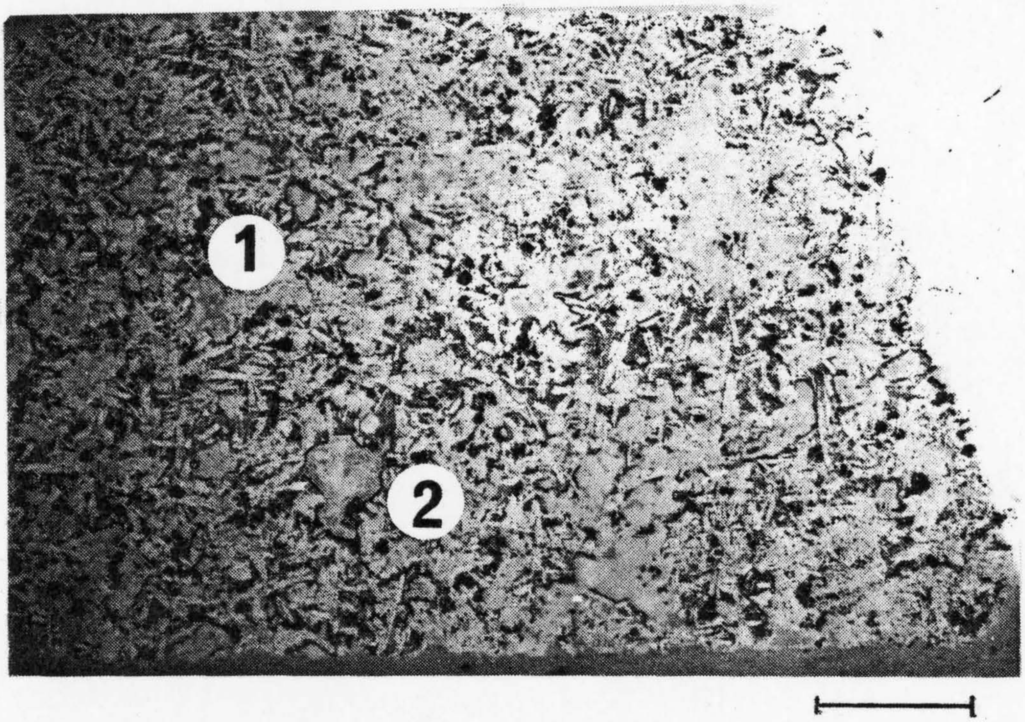

Plate 8b

relative to other minerals. The lowest concentration of B(Li) corresponds to the plagioclase and clinopyroxene grains.

Chlorite, calcite and quartz within the amygdules are low in B(Li), however the rims of these amygdules, when present, are enriched (Plate 8b, site 2). Close inspection of the rims reveals that the chlorite, not the chalcedony, has the highest affinity for B(Li).

4.2.9 The Dyke Sample (R95)

This sample consists of plagioclase laths up to 0.35 mm, clinopyroxene grains up to 0.1 mm and opaque iron-oxides up to 0.2 mm. Interstitial chlorite ± glass also occurs throughout the rock.

This specimen is relatively fine-grained with the clinopyroxene interspersed among the plagioclase laths and opaques. The plagioclase laths give a hint of preferred orientation suggesting flow texture. The overall texture of the rock is hypidiomorphic granular -- all the grains being approximately the same size. This makes the rock look fairly homogeneous in hand specimen.

The modal analysis for the minerals in the rock is presented below.

Plate 9. Sample R95: 9a, thin section; 9b, ATI; scale bar 5 mm.

B = 10.1 ppm (Table 3.4)

Li = 22.00 ppm

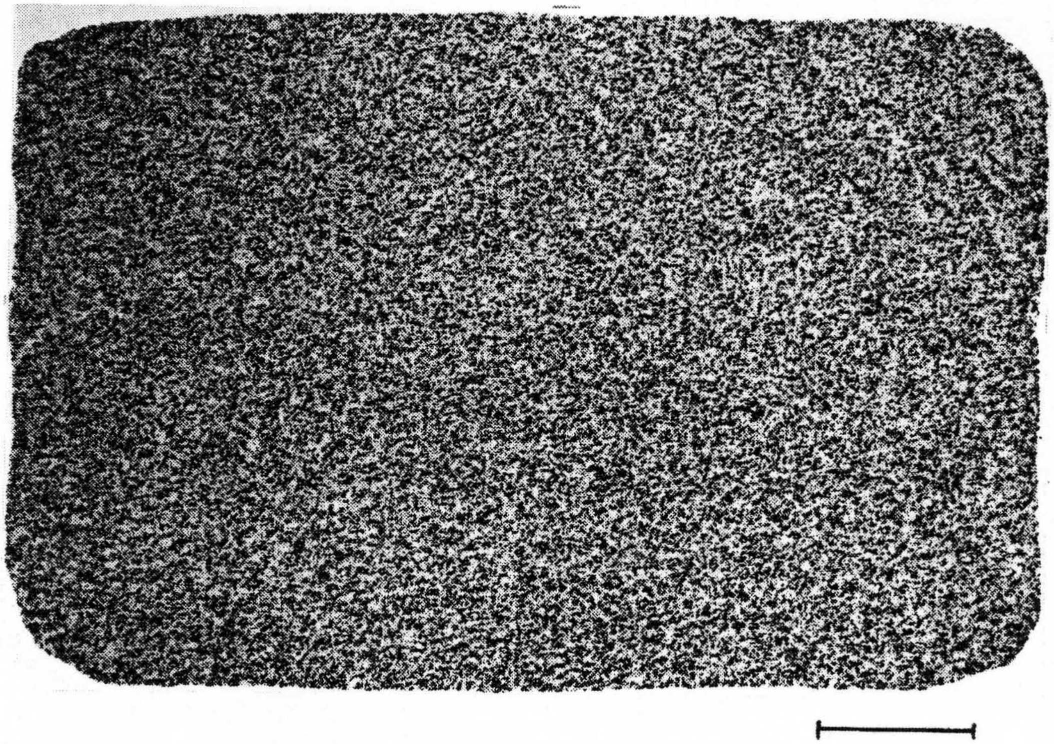

Plate 9a

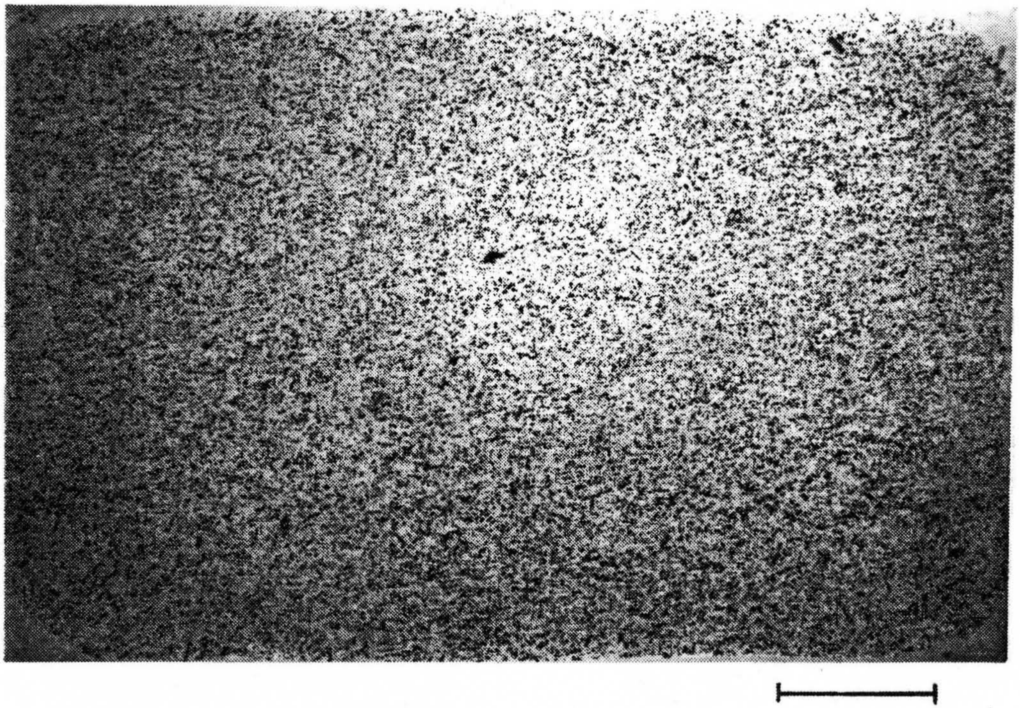

Plate 9b

	Mineral	Abundance
Primary:	Plagioclase	35%
	Clinopyroxene	30%
	Opaques (Fe-oxide)	30%
	Glass	3%
Secondary:	Chlorite	2%

Due to the fine-grained nature of this sample, it is difficult to correlate B(Li) concentration with mineralogy. B(Li) is probably associated with the opaque minerals and chlorite as there is no observable evidence to suggest otherwise.

4.3 SUMMARY

The alpha-track images of these metabasites indicate that boron is concentrated in eight different locations listed in decreasing order of importance.

1. Iron-oxide

Boron is highly concentrated in many iron oxide grains. Only a few showed low B(Li) content (e.g. sample R92, Plate 7b).

2. Chlorite

Several kinds of chlorite were found throughout these rocks representing several generations. Most of the chlorite shows high B(Li) concentration with dense tracks, however certain varieties gave weak B(Li) tracks (e.g. Plate 3b, site 1; sample R92).

3. Along microscopic fractures

Boron is concentrated in fractures of plagioclase and clinopyroxene presumably being associated with secondary alteration minerals (e.g. Plate 5b, site 1).

4. Stilpnomelane

The mineral is usually coarse-grained and gave medium B(Li) tracks (e.g. Plates 2b, 7b).

5. In an unknown mineral

This mineral was observed in sample R92 and could not be positively identified. However, it gave very intense B(Li) tracks (Plate 7b, site 3). Prehnite, danburite and datolite are possibilities for this mineral.

6. In secondary alteration phases of plagioclase (albite and epidote

Several small point concentrations of boron were observed on the plagioclase grains themselves which were not associated with fractures, but could be secondary alteration phases.

7. In plagioclase and pyroxene

These minereals were considerably lower in B(Li) concentration than most other minerals in all specimens studied.

8. In calcite and quartz (chalcedony)

These low temperature secondary phases were even lower than boron concentrations in plagioclase and clinopyroxene (e.g. Plate 3b, site 2).

It is noteworthy that no discrete grains of borosilicates occurred (unless it is the unknown mineral) in these samples. Most of the boron occurs in secondary phases.

CHAPTER 5

INTERPRETATION

5.1 ORIGIN OF THE MAMAINSE POINT FLOWS AS SUGGESTED BY BORON ENRICHMENT

5.1.1 Boron Enrichment in the Mamainse Point Flows Versus Other Basalts

The distribution of boron in the oceanic lithosphere has been studied by Bergeron (1985). His data are summarized in Table 5.1 and a comparison of these values to the Mamainse Point data (Table 3.4) shows boron enrichment relative to fresh basalts in the Mamainse Point rocks. In fact every sample studied has a higher concentration of boron than the value reported for fresh basalt. Sample R19 had the lowest boron content with approximately 4.21 ppm (Table 3.4). However, basalts from the upper surface of the oceanic crust, DSDP cores and the Troodos ophiolite (Table 5.1) all show higher boron concentrations than the Mamainse Point samples.

It is well known that seawater alteration of basalt results in boron enrichment. The concentration of boron in

Table 5.1 Boron concentrations in various fresh and altered basalts

Rock Type	Mean Boron conc. (ppm)	No. of analyses	Comments
Fresh basalt	2.9	8	--
Basalts from upper surface of oceanic crust (max 10 m depth)	13.0	22	The boron concentration is derived from analyses of dredged basalts and shallow (10 m) cores. Samples from MAR and "Blanco" Trough
DSDP (leg 37)	10.6	21	Samples taken from sites 332B and 334 of the DSDP. Cores are approximately 300 m in depth
Troodos ophiolite (Cyprus)	52.0	28	Max depth of coring is 445 m (approximately). Sequence shows decreasing [B] with increasing depth

(Data from Bergeron, 1985)

ambient seawater is approximately 4.6 ppm (Seyfried et al., 1984) and has remained stable for the last 2 - 3 billion years (Reynolds, 1965). Spooner and Fyfe (1973), Lister (1973, 1974) and Wolery (1978) report that mid-ocean ridge hydrothermal systems are recharged by geographically dispersed limbs of hot fluids through fissure systems. Seyfried et al. (1984) suggested that the descending limb of the submarine geothermal system may involve boron removal and in this way boron enrichment can occur.

Bergeron (1985) studying the Troodos ophiolite and Cyprus found a maximum enrichment of 150 ppm B. He also found that the concentration of boron decreased with depth with a surface concentration of 150 ppm B to only 8 ppm B at 500 m or greater. The surface basalts were found to be highly altered to smectite (a boron adsorber). At depth, the basalts had less smectite alteration due to a decrease in the water/rock ratio, corresponding to a decrease in boron retention. Bergeron (1985) emphasized from his studies that the two key factors which control basalt alteration are in fact the texture of the basalt and the water/rock ratio.

5.1.2 Evidence for a Non-marine Origin of the Mamainse Point Flows

A plot of B versus Fe^{3+}/Fe^{2+} has been made in Figure

Figure 5.1. B versus Fe^{3+}/Fe^{2+} for the study samples of the Mamainse Point Formation. Fe data were obtained from Massey (1980).

Plot of Fe 3+/ Fe 2+ vs. Boron conc.

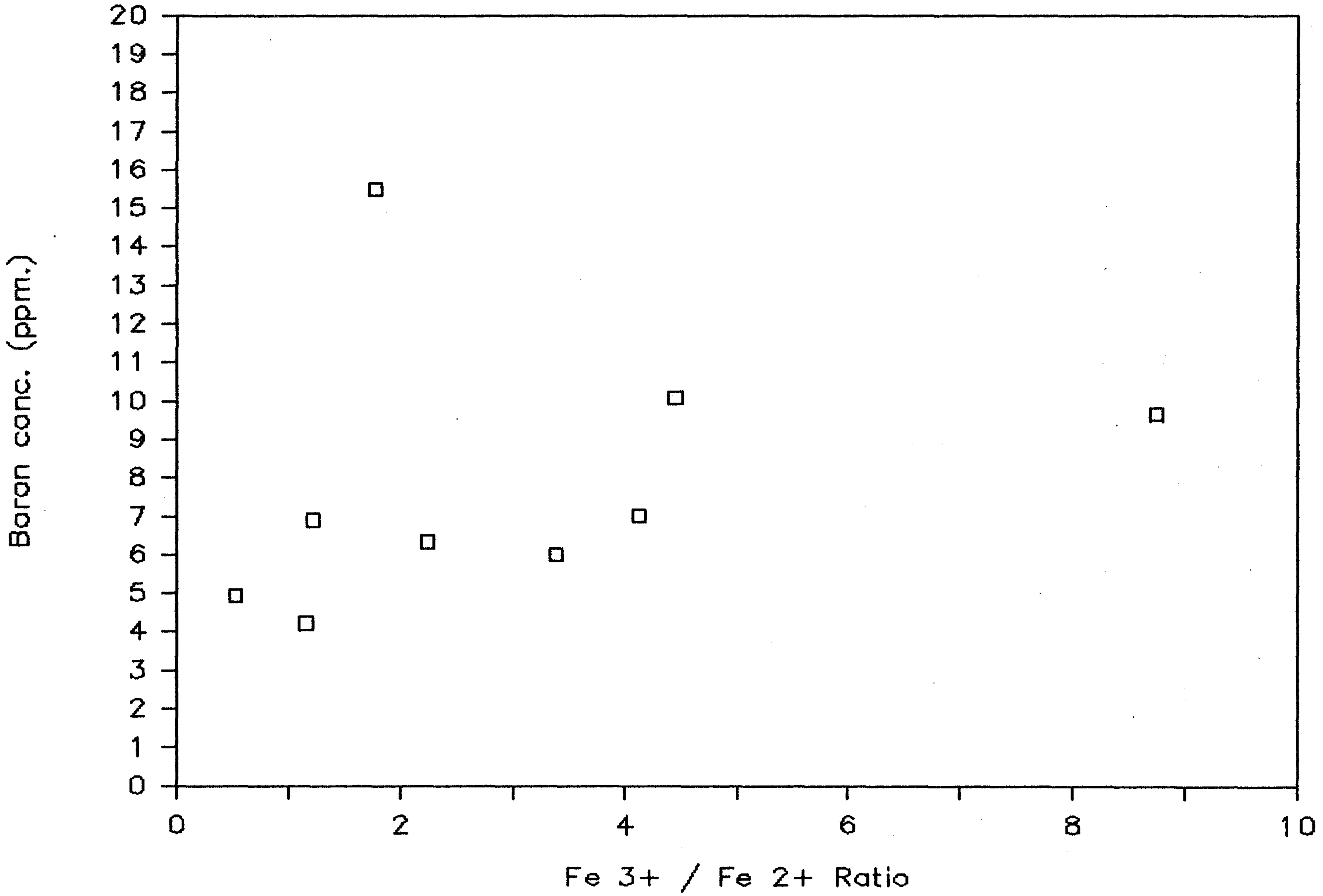

5.1. Bergeron (1985) indicated that the ratio of Fe^{3+} to Fe^{2+} was an indicator of the degree of alteration. A ratio of $Fe^{3+}/Fe^{2+} < 0.5$ indicates relatively fresh basalts while $Fe^{3+}/Fe^{2+} > 1.0$ indicates highly altered basalts. For low temperature alteration of the oceanic crust, Bergeron noted a strong positive correlation between B and Fe^{3+}/Fe^{2+}. This is not evident from Figure 5.1. A second plot, B versus H_2O^+, was made for the Mamainse Point samples (Fig. 5.2). Bergeron (1985) reports that H_2O^+ is another indicator of the degree of alteration and that low temperature alteration of the oceanic crust shows a strong positive correlation between boron and H_2O^+. However, from Figure 5.2 it can been seen that this type of relationship for the Mamainse Point samples does not exist. The Mamainse Point samples also lack the decrease in boron concentration with increasing depth reported in the Troodos ophiolite. The above arguments coupled with the lack of pillow structures and the presence of ropey pahoehoe surfaces on the Mamainse Point flows suggests that the flows are not of marine origin. They are thought to represent terrestrial or subaerial emissions.

5.1.3 Boron and the Mamainse Point Hydrothermal Cell

The hypothesis of a non-marine origin does not exclude the possibility of reactions with subsurface brines

Figure 5.2. B versus H_2O^+ for the study samples of the Mamainse Point Formation. H_2O^+ data were obtained from Massey (1980).

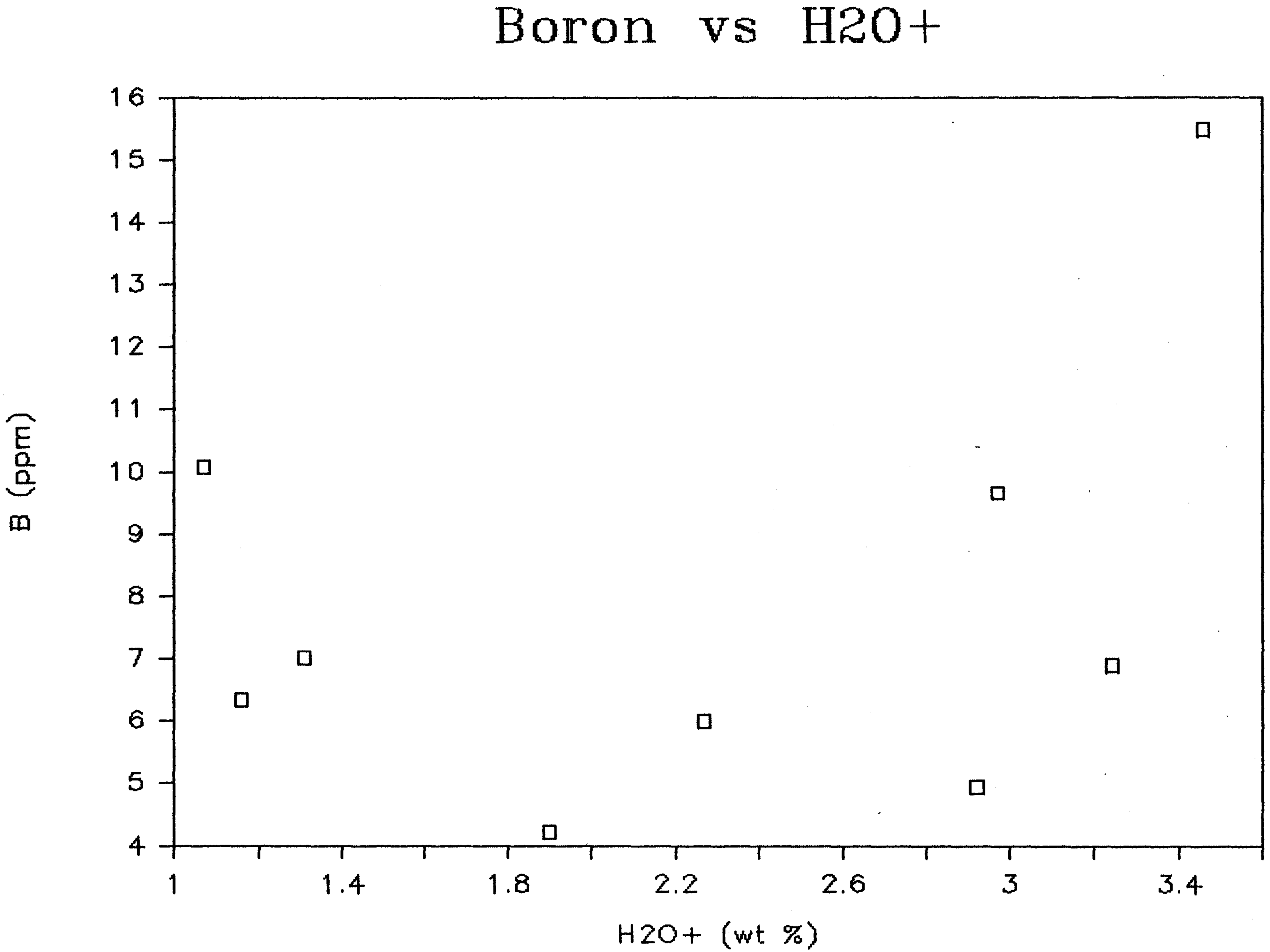
Boron vs H2O+
B (ppm)
16
15
14
13
12
11
10
9
8
7
6
5
4
1
1.4
1.8
2.2
2.6
3
3.4
H2O+ (wt %)

due to the presence of a semi-arid climate and possible drainage into the rift valley (Massey, 1980). In areas of anomalously high heat flow, geothermal convection systems can be generated by the penetration of meteoric waters through a permeable crust to the level of cooling magmatic systems (Henley and Ellis, 1983). Therefore a hydrothermal system could have acted on the Mamainse Point Formation being ultimately driven by extensive volcanism (Massey, 1980).

Many authors (Humphris and Thompson, 1978; Donnelly _et al_., 1979) have noted the large changes in boron and lithium concentrations due to hydrothermal alteration and seawater weathering of basalts from the sea floor relative to their unaltered counterparts. It has subsequently been shown by Seyfried _et al_. (1984) that boron and lithium are enriched in basalts altered by seawater at low temperatures (ref 150° C) but are leached from basalts during higher temperature alteration (ref 375°C).

Massey (1980) has reported a crude mineral zonation for the Mamainse Point Formation with epidote mineralization at the base and stilbite mineralization at the top. Epidote is known to form at higher temperatures than stilbite suggesting that higher alteration temperatures developed at the base of the volcanic pile than the top. Massey (1980) has suggested that the temperature at the peak of alteration rose to approximately 300°C and that the pressure was 2.0 to 2.5 kb. This pressure and temperature correspond to the metamorphic facies range observed at Mamainse Point. The presence of epidote and other high temperature minerals further up in the pile probably result from fluid conduits which have allowed the access of higher temperature solutions.

Shaw et al. (1986) have estimated that the surface composition of the Canadian Precambrian Shield with respect to boron is 9.2 ppm. Boron is a soluble element during hydrothermal alteration of igneous rocks and sediments (Ellis and Mahon, 1964); it is not controlled by temperature and pressure dependent solution-mineral equilibria, but primarily by its abundance in the host rock and the effective water/rock mass ratio (Seyfried et al., 1984). Boron will then partition into solution with the dissolution of primary rock minerals (Ellis and Mahon, 1984; Seyfried et al., 1984). Ground and surface waters flowing through the Archean highlands bordering the Lake Superior basin could therefore entrain boron through the weathering of these rocks, introducing it to the Mamainse Point hydrothermal system. Truscott et al. (1986) also report that boron is concentrated in the lower continental crust to approximately 2.8 ppm. This is then another boron source for circulating ground waters.

Hot, magmatic water associated with volcanism would mix with the influx of meteoric water along the margins of upward moving convection plumes (Henley and Ellis, 1983) causing boron to enter solution as an aqueous ion (commonly $B(OH)_3$ or $B(OH)_4^-$). Some boron may already be present in the hot magmatic waters due to reactions with country rock and influx of boron-containing juvenile solutions whose ultimate source is related to the degassing of the earth's mantle (Thompson and Melson, 1970).

The hydrothermal fluids flushed through the Mamainse Point Formation and a geothermal gradient at the peak of metamorphism of 40 - 50°C/km acting over the 6 km depth of the sequence would not produce a high enough temperature to preclude boron removal from solution, partitioning it into favourable solid alteration phases.

5.1.4 Dual Alteration Fluid Hypothesis and Boron Enrichment

The low grade metamorphism of the Mamainse Point Formation has been penecontemporaneous with eruption and Massey (1980) suggests that two geochemical/metamorphic events have occurred. The first, a relatively high temperature event, resulted in the hydration of the rocks as well as the addition of alkalis (Na and Li) with some oxidation of Fe. This event established epidote - chlorite

- albite assemblages. Waning burial metamorphism with decreased temperatures led to the second event causing the development of the calcite - laumontite assemblages with the remobilization of Ca and Sr. These fluids caused further oxidation of Fe and the addition of some U (Massey, 1980).

With the decrease in temperature of the solutions it would be possible for aqueous boron compounds to be removed from solution at favourable sites (chlorite, stilpnomelane and hydroxy ferric oxides).

The length of time between the two events is not positively known and depends upon whether the two fluids had separate origins or if they represent one fluid which has evolved through time. Massey (1980) also suggests that the mobilities of certain elements appear to be produced by either one or the other of the events (e.g. Li added during hydration; Ca mobilized during carbonation). Which of Massey's two events concentrated the boron is still undetermined.

5.1.5 The Composition of the Mamainse Point Source Rocks and the Access of Boron to the Formation

Seyfried and Dibble (1980), Janecky and Seyfried (1980) and Janecky (1982) have documented boron removal from solution during seawater - peridotite experiments at 200 - 300 °C and 500 bars. Thompson and Melson (1970) have studied peridotite rocks in the oceanic crust and have found that serpentinization of these rocks has resulted in the addition of boron.

The enrichment of boron in the Mamainse Point Formation favours the garnet - lherzolite source rock composition proposed by Massey (1980). These rocks are not serpentinized in the crust which would feasibly allow boron to remain in solution until it encountered the Mamainse Point Formation. Subsequent cooling of the solution would allow boron uptake.

5.1.6 Boron Uptake in the Alteration Phases of the Mamainse Point Flows

An important aspect which determines if boron will be removed from solution is alteration phase chemistry (Seyfried et al., 1984). It is important that a sink for boron be present. In the Mamainse Point samples, there are ample sites for boron uptake. From alpha-track imaging, the major sites are iron-oxide (magnetite oxidized to hematite), chlorite, stilpnomelane and microscopic fractures. Thus the boron in the Mamainse Point samples has a strong affinity for the late stage alteration minerals rather than the rock forming minerals suggesting that boron uptake is related to circulating fluids, similar to the result reported by Truscott et al. (1986), and that the concentration of boron depends on the presence of hydrous and/or hydroxy alteration products.

The dominant mechanism by which boron is removed from seawater is adsorption by continentally derived clay minerals (Seyfried et al., 1984). In dealing with clay minerals, the ions in the interlayer sites have a much greater tendency to exchange with ions in the surrounding media compared to ions in the octahedral or tetrahedral sites (Mosser, 1983). However boron, as well as lithium and strontium, have strong affinities for the latter structural sites and these elements have often been used to make interpretations of the genetic origin of clays (Mosser, 1983). Rhoades et al. (1970) reported that significant amounts of boron can be adsorbed onto $Mg(OH)_2$ (brucite) surfaces. The boron uptake occurs in two steps according to Bergeron (1985):

(1) initial adsorption of boron onto the surface of the clay

(2) slow boron diffusion into the crystalline layered structure of the clay.

Chlorite ($(Mg,Fe,Al)_{12}$ $[(Si,Al)_8 O_{20} (OH)_{16}$), found throughout the Mamainse Point Formation, is a non-expandable clay which contains the desired $Mg(OH)_2$ layer favouring boron adsorption. Lithium adsorption on chlorite is also quite possible; however, making the interpretation of the alpha-track image of this mineral a little vague.

Stilpnomelane, found in many of the flows, is another chemically complex layered structure closely related to talc. It consists of talc-like units which are separated by composite layers each consisting of sheets of iron, magnesium and aluminum ions. Being a hydrated/hydroxy compound boron adsorption in the interlayer sites is feasible.

The hydrothermal solutions which altered the Mamainse Point lavas were oxidizing (Massey, 1980). This caused the oxidation of primary iron oxides, namely magnetite (Fe_3O_4), to hydrous ferric oxides; a composition favouring the retention of boron (Sims et al., 1968). Intergrades (e.g. FeO(OH)) between $Fe(OH)_3$ and $Fe_2O_3 \cdot nH_2O$ are possible and the adsorption of naturally occurring boron compounds on these species can easily occur. However, as precipitates of iron oxides age, the degree of crystallinity increases and their surface area decreases (McPhail et al., 1972). This leads to low boron adsorption capacities, suggesting that the boron in the Mamainse Point samples was introduced into the rock by the oxidizing fluids during the period of alteration.

Sims et al. (1968) have proposed several mechanisms by which boron can be adsorbed onto hydroxy iron compounds. Two examples are shown below.

(1)

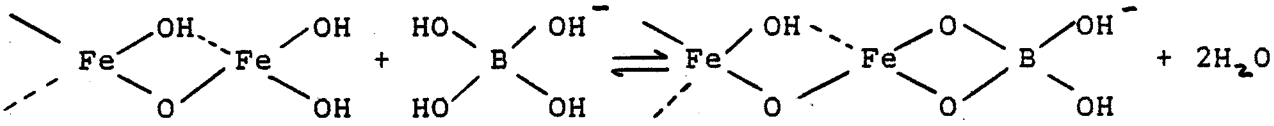

Borate ($B(OH)_4^-$) anions, which occur in more basic solutions than $B(OH)_3^0$, can continue with hydrous ferric oxides to form the end member of hydroxy iron polymers with the liberation of water.

(2)

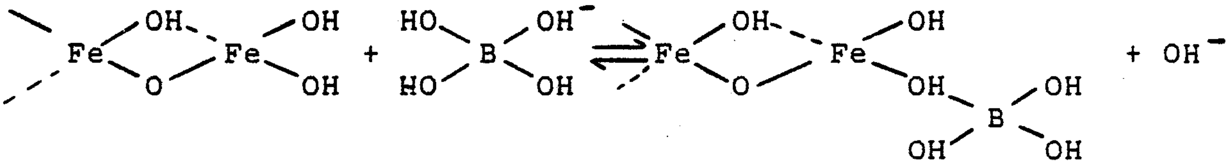

This simple exchange of borate anions for hydroxyl anions is also possible.

There are many other factors which must also be considered in light of boron adsorption. These are pH, salinity, concentration and effects of other chemical species. Each will be breifly discussed.

The adsorption of boron is pH dependent, with the maximum adsorption onto iron hydroxides occurring at pH 8.5 (McPhail <u>et al</u>., 1972). In this case boron adsorption actually increases over the pH range of 7 to 8.5 being related to increases in the increases in the number of active adsorbing sites, both of which occur in this range. Boron adsorption decreases above pH 8 or 9 due to increases in the hydroxyl ion concentration resulting in competition for adsorption sites. Also, in the case of hydroxy iron compounds, which contain Fe-OH-Fe and Fe-O-Fe linkages, ample sites for the formation of hydrogen bonds for molecular boric acid exist well into the acid pH range (down to pH 4) (Sims et al., 1968). Since the iron hydroxides of the Mamainse Point Formation are enriched in boron, the pH of the hydrothermal fluids must have been in the "neutral" range (4 - 9) and most likely in the pH range of 7 to 9.

Working with synthetic adsorbents (activated carbon, activated bauxite and activated alumina) Choi et al. (1979) found that boron removal efficiency (ability to remove B from solution) decreases fairly sharply with increasing salinity up to 8% , and then remains constant. Bingham and Page (1971) stated that boron may have preferred adsorption sites and the lack of salinity effects above 8% may be due to the filling of non-specific sites. It is quite probable that the salinity of the Mamainse Point hydrothermal fluids was greater than 8% such that it is not of major importance in the boron adsorption of these rocks.

Boron removal efficiency decreases fairly sharply with the initial concentration of boron up to a limit, above which the removal efficiency decreases very slowly with initial concentration (Choi et al., 1979).

Choi et al. (1979) also examined the effects of other chemical species and found that for many competing chemical species (e.g. Ca^{2+}, Mg^{2+}, Na^{+}, SO_4^{2-} and monosilicic acid) the removal of boron from solution decreased with increasing concentration of chemical species only to certain values after which they became unchanged. This would indicate once again that there are two types of adsorption sites: non-specific and boron specific.

Therefore, even though the hydrothermal fluids which altered the Mamainse Point lavas were quite complex it was still feasible for boron to be removed from an enriched solution by favourable hydrous and hydroxy adsorbents.

5.2 SUMMARY

The Mamainse Point lavas were erupted in a terrestrial or subaerial environment as a result of crustal rifting. The mantle source of these rocks had a garnet-lherzolite composition. Penecontemporaneous hydrothermal and burial metamorphism have caused low grade zeolite to sub-greenschist facies assemblages.

Surface and ground waters containing boron and dissolved minerals from the surrounding Archean terrain drained into the rift valley and mixed with magmatic waters associated with extensive volcanism forming a hydrothermal cell. The high temperature of the resulting fluids led to the partitioning of boron into solution as an aqueous phase.

Subsequent cooling and circulation of fluids through the Mamainse Point Formation led to boron removal from solution with adsorption onto hydrated and/or hydroxy secondary mineral phases which would favour anion exchange processes.

The highly oxidized nature of the intercalated sediments of the Mamainse Point Formation suggests that they acted as conduits for the diagenetic fluids. Fractures in the lavas would also allow fluid penetration.

Therefore, the lavas of the Mamainse Point Formation became enriched in boron relative to fresh basalts. The lack of a serpentinized peridotite mantle favours boron access to the lava sequence.

REFERENCES

ANNELLS, R.N., 1971. Keweenawan volcanics of Eastern Lake Superior. in Report of Activities, Part A: April to October, 1970. Geol. Surv. Can. Paper 71-1A, 116-119.

ANNELLS, R.N., 1973. Proterozoic flood basalts of Eastern Lake Superior: the Keweenawan volcanic rocks of the Mamainse Point area, Ontario. Geol. Surv. Can. Paper 72-10.

ANNELLS, R.N., 1974. Keweenawan volcanic rocks of Michipicoten Island, Lake Superior, Ontario. Geol. Surv. Can. Bull. 218.

BENNETT, G.D., 1967. Ontario Department of Mines, Misc. Paper, 10.

BERGERON, M., 1985. La distribution et le comportement du bore dans la lithosphere oceanique. Unpub. Ph.D. thesis, McMaster University, Hamilton, Ontario.

BINGHAM, F.T. and PAGE, A.L., 1971. Specific character of boron adsorption by an amorphous soil. Soil Sci. Amer. Proc., 35(6), 892-893.

BOOKS, K.G., 1972. Paleomagnetism of some Lake Superior Keweenawan rocks. U.S. Geol. Surv. Prof. Paper 760, 42p.

BURKE, K.C., 1978. Continental Rifts. 1978 International Symposium. Rio Grande Rift, Prog. and Abstr., 21-22.

BURKE, K.C. and DEWEY, J.F., 1973. Plume generated triple junctions: key indicators in applying plate tectonics to old rocks. J. Geol. 81, 406-433.

CHOI, W.W. and CHEN, K.Y., 1979. Evaluation of boron removal by adsorption on solids. Environ. Sci. Tech. 13, 189-196.

DAVIDSON, D.M., Jr., 1982. Geological evidence relating to interpretation of the Lake Superior basin structure. Geol. Soc. Amer. Memoir 156, 47-55.

DONNELLY, T.W., PIRCHARD, R.A. and EMMORMAN, R., 1979. The aging of the oceanic crust: synthesis of the mineralogic and chemical results of DSDP, Legs 51 through 53. in Initial Reports of the Deep Sea Drilling Project, vol. 51, 52, 53, Part 2 (eds. T. Donnelly, J. Francheteau, W. Bryan, P. Robinson, M. Flower, M. Salisbury et al.), 2563-2577. U.S. Gov't. Printing Office, Washington, D.C.

ELLIS, A.J. and MAHON, W.A.J., 1964. Natural hydrothermal systems and experimental hot-water/rock interactions (Part II). Geochim. Cosmochim. Acta 31, 519-538.

GIBLIN, P.E., 1969. Ontario Dept. of Mines. Maps P553, P554, P555, P556.

GREEN, J.C., 1971. The North Shore Volcanic Group, field guide. 17th Ann. Inst. Lake Superior Geol. Proc., 73-96.

GREEN, J.C., 1977. Keweenawan plateau volcanism in the Lake Superior region. in Volcanic Regimes in Canada (eds. W.R.A. Baragar, L.C. Coleman and J.M. Halls), 407-422. Volcanic Regimes in Canada, Spec. Paper 16.

GREEN, J.C., 1982. Geology of Keweenawan extrusive rocks. Geol. Soc. Amer. Memoir 156, 47-55.

HALLS, H.C., 1966. AGU Mono. 10, 3.

HALLS, H.C., 1978. The Late Precambrian central North American rift system -- a survey of recent geological and geophysical investigations. in Tectonics and Geophysics of Continental Rifts (eds. I.B. Ramberg and E.R. Neuman), D. Reidel, Dordrect, 111-123.

HENLEY, R.W. and ELLIS, A.J., 1983. Geothermal systems, ancient and modern: a geochemical review. Earth Sci. Rev. 19, 1-50.

HIGGINS, M.D., TRUSCOTT, M.G., SHAW, D.M., BERGERON, M., BUFFET, G.H., COPLEY, J.R.D. and PRESTWICK W.V., 1984. Prompt Gamma Neutron Activation Analysis at the McMaster Nuclear Reactor. in Use and Development of Low and Medium Flux Research Reactors (eds. O.K. Harling, L. Clark and P. von der Hardt), 690-697. Supplement to vol. 44 Atomkern-Energie Kerntechnik.

HUMPHRIS, S.E. and THOMPSON, G., 1978. Trace element mobility during hydrothermal alteration of oceanic basalts. Geochim. Cosmochim. Acta 42, 127-137.

IRVINE, T.N. and BARAGAR, W.R.A., 1971. A guide to the chemical classification of the common volcanic rocks. Can. J. Earth Sci. 8, 523-548.

JANECKY, D.R., 1982. Serpentinization of peridotite within the oceanic crust: Experimental and theoretical investigations of seawater-peridotite interaction at 200 C and 300 C, 500 bars. Ph.D. dissertation, University of Minnesota, 244p.

JANECKY, D.R. and SEYFRIED, W.E. Jr., 1980. Seawater peridotite interaction: chemical exchange and secondary mineral formation. in Third International Symposium on Rock-Water Interaction, Edmonton, 173-175.

JIRSA, M.A., 1978. The petrology and tectonic significance of interflow sediments in the Keweenawan North Shore Volcanic Group of northwestern Minnesota (abstr.). 24th Ann. Inst. on Lake Superior Geol., Milwaukee, WI, p.17.

JOLLY, W.T., 1974. Behavior of Cu, Zn and Ni during prehnite-pumpellyite rank metamorphism of the Keweenawan basalts, Northern Michigan. Econ. Geol. 69, 1118-1125.

JOLLY, W.T. and SMITH, R.E., 1972. Degradation and metamorphic differentiation of Keweenawan Tholeiitic lavas of Northern Michigan, U.S.A. J. Petrol. 13, 273-309.

KING, E.R. and ZIETZ, I., 1970. Aeromagnetic study of the mid-continent gravity high of the central United States. Geol. Soc. Amer. Bull. 82, 2187-2208.

LISTER, C.R.B., 1973. Hydrothermal convection at seafloor spreading centres: source of power or geological nightmare? (abstr). Abstract with Programs, Geol. Soc. Amer. Ann. Mtg. (Cordilleran Section) 5, p.74.

LISTER, C.R.B., 1974. On the penetration of water into hot rock. Geophys. J. Roy. Astron. Soc. 39, 465-509.

MASSEY, N.W.D., 1979. Keweenawan paleomagnetic reversals at Mamainse Point, Ontario: Fault repetition or three reversals? Can. J. Earth Sci. 16, 373-375.

MASSEY, N.W.D., 1980. The geochemistry of some Keweenawan metabasites from Mamainse Point, Ontario. Unpub. Ph.D. thesis, McMaster University, Hamilton, Ontario.

McPHAIL, M., PAGE, A.L. and BINGHAM, F.T., 1972. Adsorption interactions of monosilicic and boric acid on hydrous oxides of iron ad aluminum. Soil Sci. Amer. Proc. 36, 510-514.

McWILLIAMS, M.O. and DUNLOP, D.J., 1978. Grenville paleomagnetism and tectonics. Can. J. Earth Sci. 15, 687-695.

MERK, G.P. and JIRSA, M.A., 1982. Provenance and tectonic significance of the Keweenawan interflow sedimentary rocks. Geol. Soc. Amer. Memoir 156, 97-105.

MOREY, G.B. and GREEN, J.C., 1982. Status of the Keweenawan as a stratigraphic unit in the Lake Superior region. Geol. Soc. Amer. Memoir B156, 15-25.

MOSSER, C., 1983. The use of boron to determine clay origin. Chem. Geol. 38, 129-140.

NICHOLLS, R.L., 1936. Flow units in basalts. J. Geol. 44, 617-630.

PEISACH, M., 1981a. Prompt techniques. in Nondestructive Activation Analysis (ed. S. Amiel), Elsevier Scientific Publishing Company, 93-112.

PEISACH, M., 1981b. Specific counting techniques. in Nondestructive Activation Analysis (ed. S. Amiel), Elsevier Scientific Publishing Company, 71-92.

REYNOLDS, R.C. Jr., 1965. The concentration of boron in Precambrian seas. Geochim. Cosmochim. Acta 29, 1-16.

RHOADES, J.D., INGNALSON, R.D. and HATCHER, J.T., 1970. Adsorption of boron by ferromagnesian minerals and magnesium hydroxide. Soil Sci. Soc. Amer. Proc. 34, 938-941.

SAWKINS, F.J., 1976. Widespread continental rifting: some considerations of timing and mechanism. Geology 4, 427-430.

SCHWARZBACH, M., 1963. Climates of the Past. von Nostrand (London, Princeton, New York, and Toronto), 328p.

SEYFRIED, W.E., Jr., JANECKY, D.R. and MOTTL, M.J., 1984. Alteration of the oceanic crust: Implications for geochemical cycles of lithium and boron. Geochim. Cosmochim. Acta 48, 557-569.

SEYFRIED, W.E., Jr. and DIBBLE, W.E., Jr., 1980. Seawater peridotite interaction at 300 C, 500 bars: Implications of the origin of oceanic peridotites. Geochim. Cosmochim. Acta 44, 309-321.

SHAW, D.M., CRAMER, J.J., HIGGINS, M.D. and TRUSCOTT, M.G., 1986. Composition of the Canadian Precambrian Shield and the continental crust of the earth. in The Nature of the Lower Continental Crust (eds. J.B. Dawson, D.A. Carswell, J. Hall and K.H. Wedepohl), 275-282. Geol. Soc. Spec. Pub. no. 24.

SIMS, J.R. and BINGHAM, F.T., 1968. Retention of boron by layer silicates, sesquioxides and soil materials: II. Sesquioxides. Soil Sci. Amer. Proc. 32, 364-369.

SPOONER, E.T.C. and FYFE, W.F., 1973. Subsea-floor metamorphism, heat and mass transfer. Contrib. Mineral. Petrol. 42, 287-304.

THOMPSON, G. and MELSON, W.G., 1970. Boron contents of serpentinites and metabasalts in the oceanic crust: Implications for the boron cycle in the oceans. Earth Planet. Sci. Lett. 8, 61-65.

TRUSCOTT, M.G., SHAW, D.M. and CRAMER, J.J., 1986. Boron abundance and localization in granulites and the lower continental crust. Bull. Geol. Soc. Finland 58, Part 1, 169-177.